Advanced I/Q Signal Processing for Communication Systems

Mikko Valkama and Markku Renfors

Tampere University of Technology
Institute of Communications Engineering
P.O.Box 553, FIN-33101 Tampere, FINLAND
Tel: +358-40-8490-756, Fax: +358-3-3115-3808
E-mail: valkama@cs.tut.fi and mr@cs.tut.fi

SDR-03 Technical Conference, Nov. 2003, Orlando, FL

CONTENTS

4. Adaptive DSP for I/Q Imbalance Compensation

- Blind signal estimation based imbalance compensation
- Simulation examples

5. Second-Order Sampling and its Enhancements

- Basic second-order sampling scheme
- Imbalance problem and image rejection
- Enhancing the image rejection using DSP

6. I/Q Signal Processing in Frequency Synthesizers

- Digitally synthesized complex tone and analog I/Q mixing
- I/Q imbalance problem revisited

Summary

References

1. COMPLEX SIGNALS AND SYSTEMS

Background and Motivation

– All physical signals and waveforms are **real-valued**

→ so why bother to consider **complex-valued** signals and systems ?

– The original complex signal concepts can be traced back to the introduction of lowpass equivalent notation, i.e., analysis of **bandpass** signals and systems using their lowpass/baseband equivalents

→ in general, a real-valued bandpass signal/system has a complex-valued lowpass equivalent

- for example, linear I/Q modulation and demodulation principles are based on these ideas
- also all advanced frequency translation techniques and thus the related receiver architectures (low-IF, direct-conversion, etc.) utilize complex signals
- sampling and efficient multirate processing of bandpass signals is another good example

Basic Concepts and Definitions

– By definition, the time domain waveform or sequence $x(t)$ of a **complex signal** is complex-valued, i.e., $x(t) = x_I(t) + jx_Q(t)$.

– In practice, this is nothing more than a pair of two real-valued signals $x_I(t)$ and $x_Q(t)$ carrying the real and imaginary parts.

– Similarly, a **complex system** is defined as a system with complex-valued impulse response.

– In the **frequency domain**, real-valued signals have always symmetric amplitude spectrum

→ complex signals don't (need to) have any symmetry properties in general

→ the spectral support (region of non-zero amplitude spectrum) can basically be anything

– One basic operation related to complex quantities is **complex-conjugation**

→ if the spectrum of $x(t)$ is denoted by $X(f)$, then the spectrum of $x^*(t)$ is $X^*(-f)$

→ this simple-looking result is surprisingly useful when interpreting some properties of complex signals in the continuation

→ an immediate consequence is that if you consider the real part of $x(t)$, i.e., $y(t) = \mathrm{Re}[x(t)] = (x(t) + x^*(t))/2$, its spectrum is $Y(f) = (X(f) + X^*(-f))/2$

- if $X(f)$ and $X^*(-f)$ are not overlapping, $y(t) = \mathrm{Re}[x(t)]$ contains all the information about $x(t)$
- this result will find good use, e.g., in understanding frequency translations

– Another key operation related to linear systems in general is **convolution**.

– In the general complex case, this can be written as

$$x(t) * h(t) = (x_I(t) + jx_Q(t)) * (h_I(t) + jh_Q(t))$$
$$= x_I(t) * h_I(t) - x_Q(t) * h_Q(t) + j(x_I(t) * h_Q(t) + x_Q(t) * h_I(t))$$

– In other words, 4 real convolutions are needed in general.

– Obvious simplifications occur if either the filter input or the filter itself is real valued

→ in these cases, only two real convolutions need to be calculated

Analytic Signals and Hilbert Transforms

– Hilbert transformer is generally defined as an allpass linear filter which shifts the phase of its input signal by 90 degrees.

– The (anticausal) impulse and frequency responses can be formulated as

continuous-time	discrete-time
$h_{HT}(t) = \frac{1}{\pi t}$	$h_{HT}(n) = \begin{cases} 0, & n \text{ even} \\ 2/(\pi n), & n \text{ odd} \end{cases}$
$H_{HT}(f) = \begin{cases} -j, & f \geq 0 \\ +j, & f < 0 \end{cases}$	$H_{HT}(e^{j\omega}) = \begin{cases} -j, & 0 \leq \omega < \pi \\ +j, & -\pi \leq \omega < 0 \end{cases}$

– In practice this behaviour can be well approximated over a finite bandwidth.

– One fascinating property related to Hilbert filters/transformers is that they can be used to construct **signals with only positive frequency content**.

– This kind of signals are generally termed **analytic** and they are always complex.

– The simplest example is to take a cosine wave $A\cos(\omega_1 t)$ whose Hilbert transform is $A\sin(\omega_1 t)$ (just a 90 degree phase shift!)

→ these together when interpreted as I and Q components of a complex signal result in $A\cos(\omega_1 t) + jA\sin(\omega_1 t) = A\exp(j\omega_1 t)$ whose spectrum has an impulse at ω_1 but nothing on the other side of the spectrum

– The "elimination" of the negative frequencies can more generally be formulated as follows.

– Starting from an arbitrary signal $x(t)$ we form a complex signal $x(t) + jx_{\mathrm{HT}}(t)$ where $x_{\mathrm{HT}}(t)$ denotes the Hilbert transform of $x(t)$.

– Then the spectrum of the complex signal is $X(f)[1 + jH_{\mathrm{HT}}(f)]$ where

continuous-time

$$1 + jH_{HT}(f) = \begin{cases} 1 + j\times(-j), & f \geq 0 \\ 1 + j\times j, & f < 0 \end{cases} = \begin{cases} 2, & f \geq 0 \\ 0, & f < 0 \end{cases}$$

which shows the elimination of the original negative frequency content. Similar concepts carry on to discrete-time world and we can write

discrete-time

$$1 + jH_{HT}(e^{j\omega}) = \begin{cases} 1 + j\times(-j), & 0 \leq \omega < \pi \\ 1 + j\times j, & -\pi \leq \omega < 0 \end{cases} = \begin{cases} 2, & 0 \leq \omega < \pi \\ 0, & -\pi \leq \omega < 0 \end{cases}$$

– This idea of using Hilbert transform to generate analytic signals is further illustrated graphically in the following figure.

– In practice the Hilbert filtering causes a delay and a corresponding delay needs to be included also in the upper (I) branch.

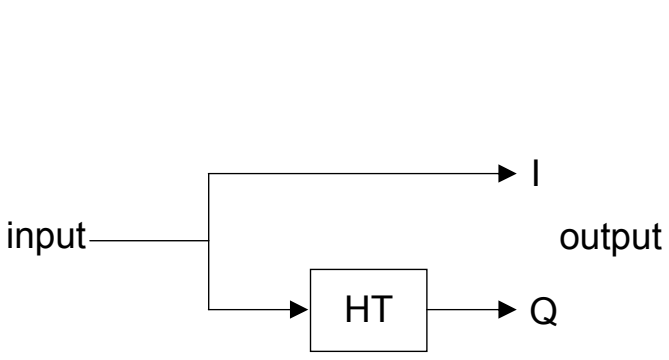

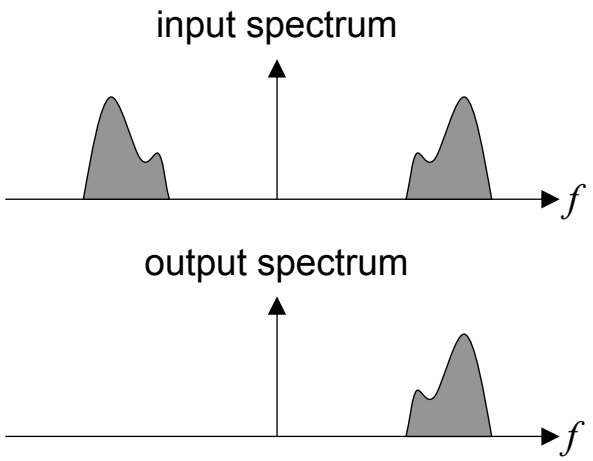

– **Design Example:** Hilbert transformer of order 50, design bandwidth 0.1π … 0.9π (π denotes half the sampling frequency), Remez design

→ this results in about 87 dB attenuation for the negative frequencies (wrt. corresponding positive band)

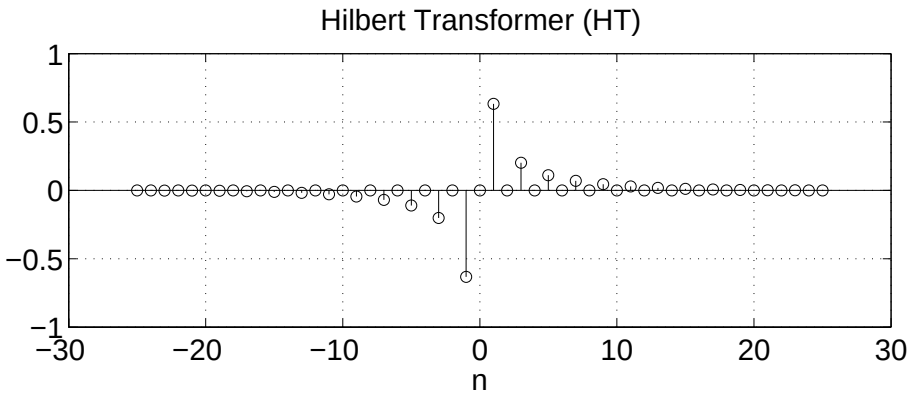

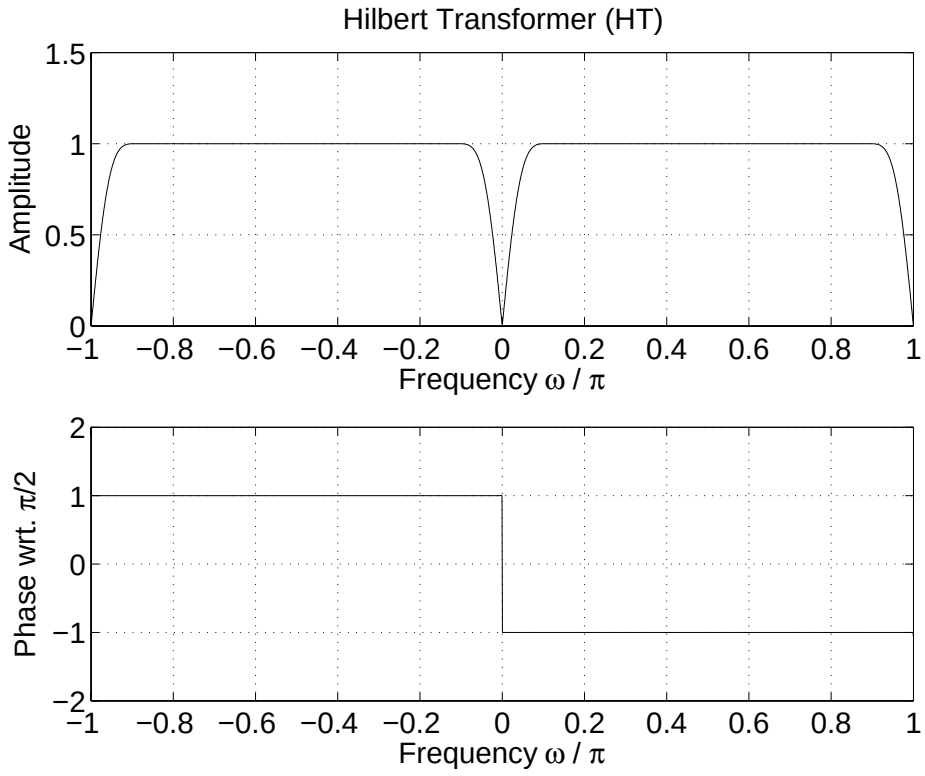

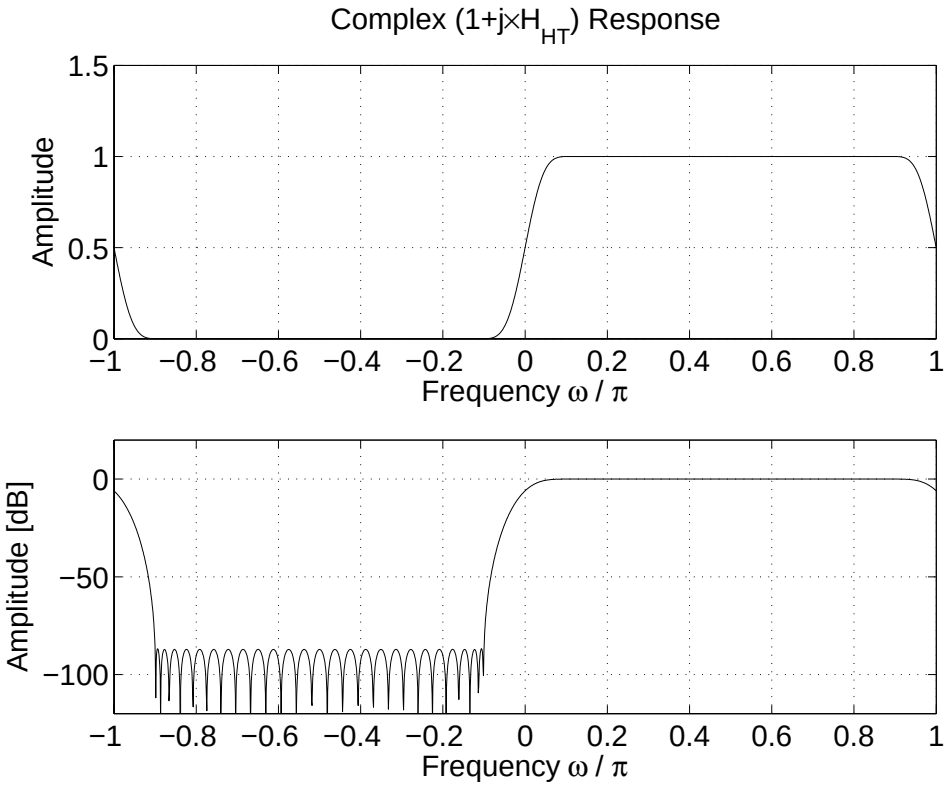

Frequency Translations and Mixing

– One key operation in communications signal processing is the shifting of a signal spectrum from one center-frequency to another

  → conversions between baseband and bandpass representations are special cases of this

– The basis of all the frequency translations lies in multiplying a signal with a complex exponential, generally referred to as **complex or I/Q mixing**.

– This will indeed cause a pure frequency shift, i.e.,

$$y(t) = x(t)e^{j\omega_{LO}t} \quad \Leftrightarrow \quad Y(f) = X(f - f_{LO})$$

  which forms the basis for all the linear modulations.

– This is illustrated in frequency domain below.

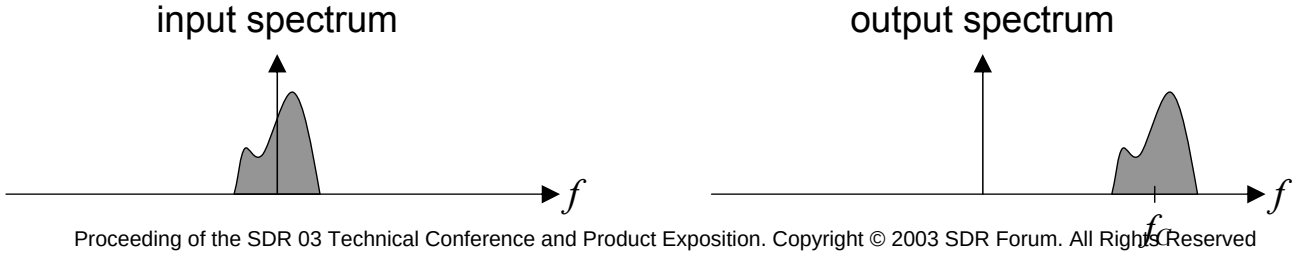

– In general, four real mixers are needed to implement a complex mixer as

$$x(t)e^{j\omega_{LO}t} = (x_I(t) + jx_Q(t))(\cos(\omega_{LO}t) + j\sin(\omega_{LO}t))$$
$$= x_I(t)\cos(\omega_{LO}t) - x_Q(t)\sin(\omega_{LO}t) + j(x_Q(t)\cos(\omega_{LO}t) + x_I(t)\sin(\omega_{LO}t))$$

→ in the special case of a real input, only two mixers needed

– **Real mixing** is obviously a special case of the previous complex one and results in two frequency translations:

$$y(t) = x(t)\cos(\omega_{LO}t)$$
$$= x(t)\frac{1}{2}(e^{j\omega_{LO}t} + e^{-j\omega_{LO}t}) \quad \Leftrightarrow \quad Y(f) = \frac{1}{2}X(f - f_{LO}) + \frac{1}{2}X(f + f_{LO})$$

– Here, the original spectral component appear twice in the mixer output, the two replicas being separated by $2f_{LO}$ in frequency.

– In receivers, this results in the so called **image signal** problem since the signals from both $f_C + f_{LO}$ and $f_C - f_{LO}$ will appear at f_C after the real mixing stage

→ if real mixing is used, the image signal needs to be attenuated before the actual mixer stage

→ we'll talk about this in more detail in the receiver architecture section

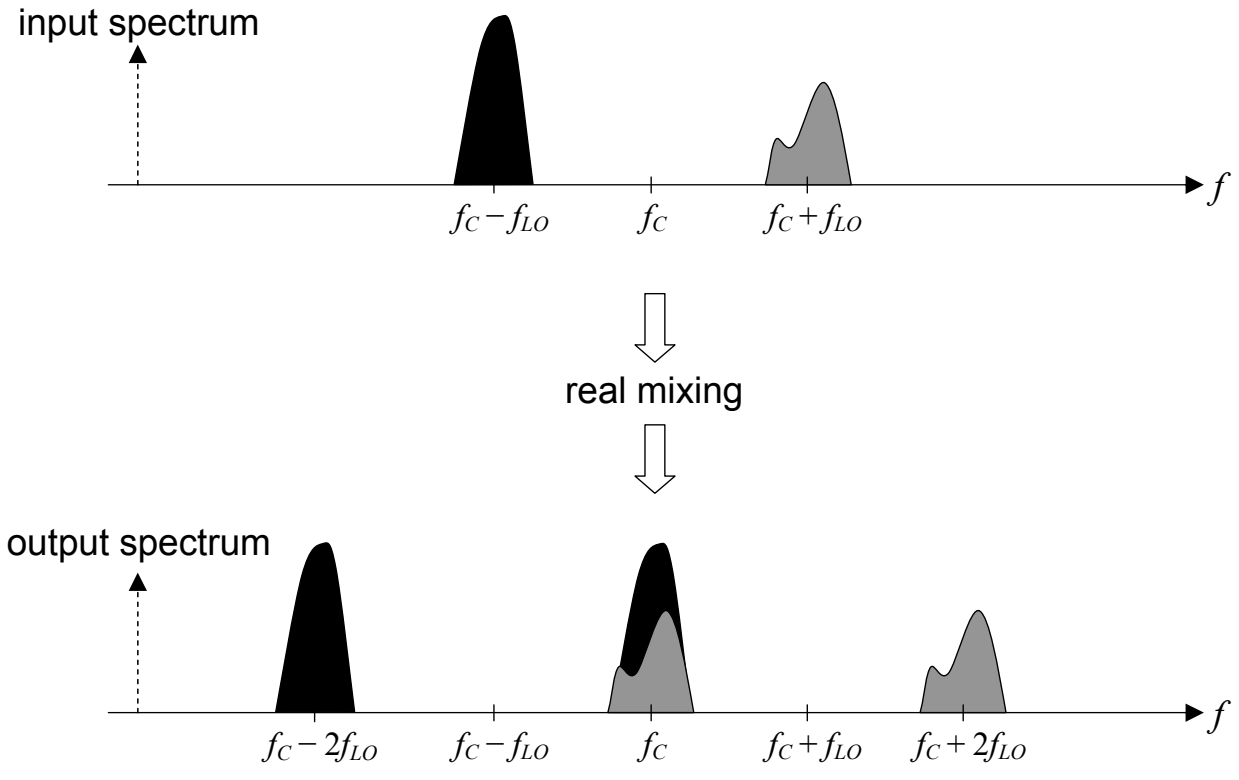

– Linear **I/Q modulation** methods are basically just a special case of complex mixing.

– Given a complex message signal $x(t) = x_I(t) + jx_Q(t)$, it is first modulated as $x(t)\exp(j\omega_C t)$, after which only the real part is actually transmitted:

$$y(t) = \mathrm{Re}[x(t)e^{j\omega_C t}] = x_I(t)\cos(\omega_C t) - x_Q(t)\sin(\omega_C t) = \frac{1}{2}x(t)e^{j\omega_C t} + \frac{1}{2}x^*(t)e^{-j\omega_C t}$$

→ interpretation #1: $x_I(t)$ and $x_Q(t)$ are modulated onto two orthogonal (cosine and sine) carriers; nice from the implementation point of view

→ interpretation #2: $x(t)$ and $x^*(t)$ are modulated onto two complex exponentials $\exp(j\omega_C t)$ and $\exp(-j\omega_C t)$; key in building general understanding and recovering $x(t)$ back from $y(t)$

– Notice that both terms/spectral components (at $+f_C$ and $-f_C$) contain all the original information (i.e., $x(t)$).

– This process, also termed lowpass-to-bandpass transformation, is pictured in the figure below.

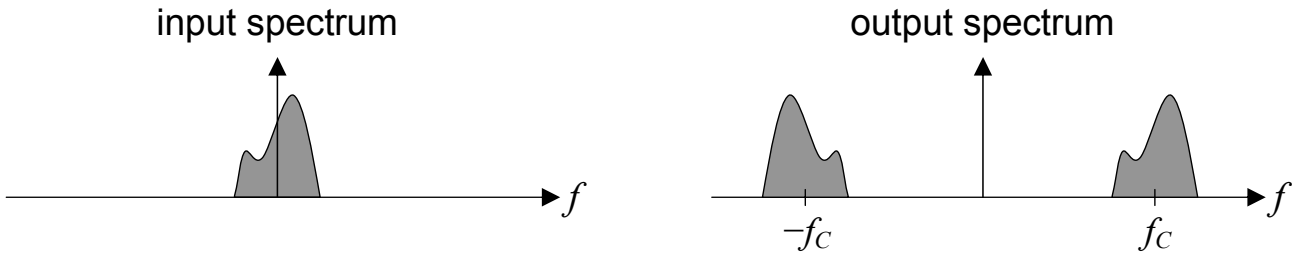

– **I/Q demodulation:** In the receiver, the goal is to recover the original message $x(t)$ from the modulated signal $y(t)$.

– Based on the previous discussion, it's easy to understand that either of the signal components at $+f_C$ or $-f_C$ can be used for that purpose, while the other one should be rejected.

– Since

$$y(t)e^{-j\omega_C t} = (\frac{1}{2}x(t)e^{j\omega_C t} + \frac{1}{2}x^*(t)e^{-j\omega_C t})e^{-j\omega_C t} = \frac{1}{2}x(t) + \frac{1}{2}x^*(t)e^{-j2\omega_C t}$$

the message can be fully recovered by simply lowpass filtering the complex receiver mixer output.

– Formal block-diagrams for the modulator and demodulator in terms of complex signals are presented below.

MODULATOR:

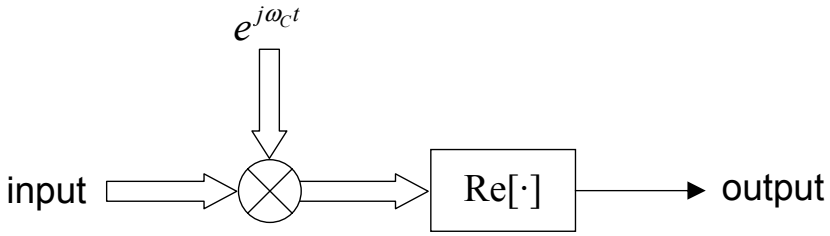

DEMODULATOR:

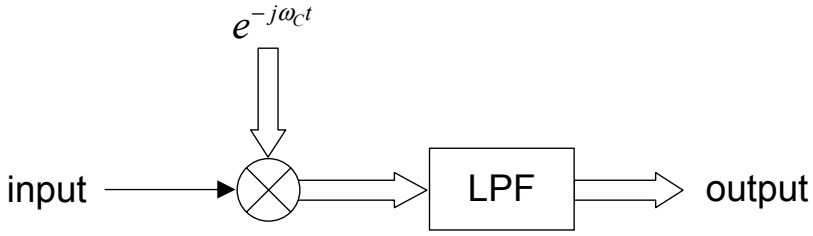

Complex Signals and Sampling

– In periodic sampling (sample rate f_S) the resulting discrete-time signal has a periodic spectrum where the original continuous-time spectrum is replicated around the integer multiples of the sampling frequency.

– Interestingly, any of these spectral replicas (or "images") can be considered as the useful part and thus be used for further processing.

– Consequently, sampling (and multirate operations in general) can also be used, in addition to mixing techniques, in performing frequency translations.

– Let B denote the double-sided bandwidth of a complex-valued baseband signal (i.e., the spectrum is nonzero only for $-B_{neg} \le f \le B_{pos}$, $B = B_{neg} + B_{pos}$)

→ to avoid aliasing, the sampling frequency f_S should simply be high enough such that the spectral images don't overlap, i.e.,

$$f_S - B_{neg} \ge B_{pos} \quad \Leftrightarrow \quad f_S \ge B_{neg} + B_{pos} \quad \Leftrightarrow \quad \underline{f_S \ge B}$$

→ this is the traditional Nyquist sampling theorem

→ naturally, since the signal to be sampled is complex-valued, there exist two real-valued sample streams (I and Q) both at rate f_S

→ if the signal to be sampled consists of multiple frequency channels, sampling rates below $f_S = B$ are possible if only some of the channels are of interest

- the sampling frequency should simply be selected in such a manner that aliasing is avoided on top of those interesting frequency bands

– Example spectra which both have the same lower limit $f_S = B$ for the sampling frequency are depicted below.

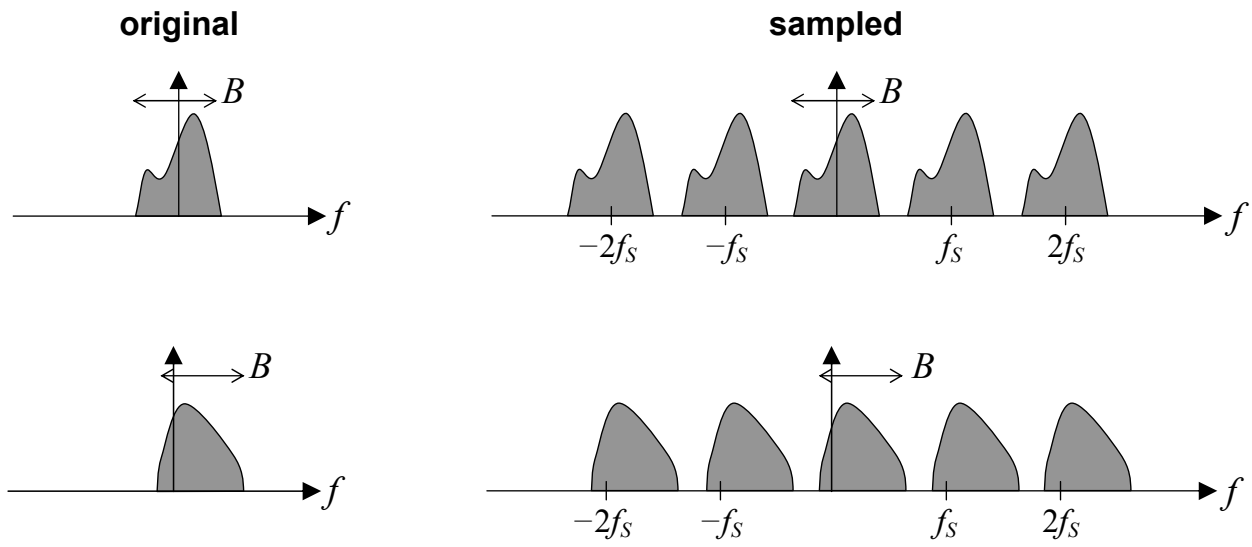

– **Conclusion:** It doesn't matter whether the signal is real or complex or whether it is located "symmetrically" with respect to origin

→ the minimum sampling rate is always $f_S = B$

– So in general the traditional statement "signal should be sampled at least at rate two times its highest frequency component" can be concluded inaccurate

→ what really matters is the double-sided bandwidth

→ a good example is the sampling of a real-valued lowpass signal, say $x(t)$, with spectral support $-W \ldots W$

- when sampled directly, the minimum sampling rate is $f_S = 2W$
- as an alternative, you can form an analytic signal $x(t) + jx_{\mathrm{HT}}(t)$, where $x_{\mathrm{HT}}(t)$ denotes the Hilbert transform of $x(t)$, for which the minimum sampling rate is only $f_S = W$ (even though the highest frequency component present in both signals is W)

2. Sampling and Multirate DSP with Bandpass and I/Q Signals

Sampling of Bandpass Signals

– Starting point is the traditional Nyquist sampling theorem: Any signal occupying the band $-B_{neg} \ldots B_{pos}$ [Hz] is completely characterized by its discrete-time samples given that the sampling rate is at least $B_{neg} + B_{pos}$ (two-sided bandwidth).

– People commonly interpret this that if the highest frequency component in a signal is f_{MAX}, you need to take at least $2f_{MAX}$ samples per second

→ strictly speaking, this is inaccurate (as concluded before)

→ i.e., sampling at or above rate $2f_{MAX}$ is clearly always sufficient but e.g. in case of **bandpass signals** we can also use (usually much) lower sample rate

→ more specifically, sampling at rate below $2f_{MAX}$ will indeed result in aliasing but as long as all the information about the original signal is present in the samples, we are doing good

- keep in mind also that the Nyquist ("accessible") band for any sample rate f_S is $-f_S/2 \ldots f_S/2$, so with below $2f_{MAX}$ sampling rates it is really one of the images that appear on this band !!!

→ these kind of techniques are generally referred to as **subsampling**

– The one and only principle to remember in sampling is that the resulting signal has a periodic spectrum and any part of that spectrum can be selected/used for further processing.

– More specifically, in communications receivers, **aliasing due to sub-sampling can be taken advantage of to bring the signal closer to baseband**.

– We consider two cases; starting from a real-valued bandpass signal, the resulting sample stream is either 1) real-valued or 2) complex-valued.

Real Subsampling

– Basic setup: real-valued bandpass signal, bandwidth B, center-frequency f_C, upper band-edge $f_U = f_C + B/2$ and lower band-edge $f_L = f_C - B/2$.

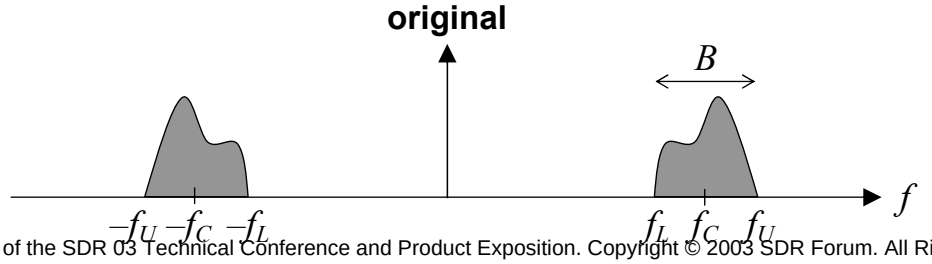

– Now sampling at some rate f_S results in a signal where the previous spectrum is replicated at integer multiples of the sampling rate (the basic effect of sampling).

– With $f_S < 2f_U$, aliasing will take place but as long as the aliasing components don't fall on top of each other, everything is OK !!

– So an example spectrum of the sampled signal could look like in the figure below, when there is no harmful aliasing and yet $f_S < 2f_U$.

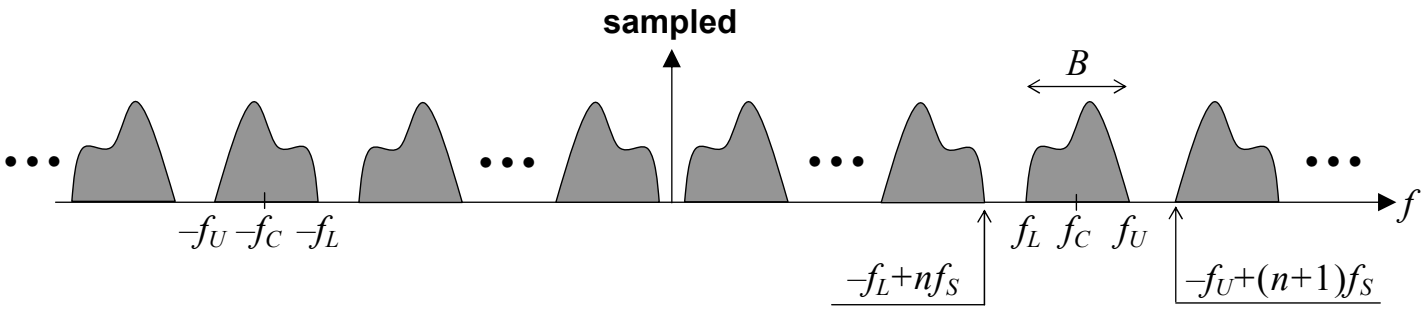

– Based on the above figure, it is easy to formulate the regions of allowable sampling rates. These are in general of the form

$$\frac{2f_C+B}{n+1} \le f_S \le \frac{2f_C-B}{n} \quad \text{where} \quad 0 \le n \le floor(\frac{2f_C-B}{2B})$$

– Comments:

→ as can be seen, the possible values of the sampling rate depend on both the **bandwidth** B and the **center-frequency** f_C

→ for $n=0$ we get $f_S \ge 2f_C+B = 2(f_C+B/2) = 2f_U$ which is the traditional Nyquist sampling theorem (the upper limit becomes infinity)

→ for $n>0$ we are really sampling at lower frequency than given by the traditional Nyquist theorem

→ for $n>0$ **aliasing does occur** but with given values of f_S, not on top of the desired signal band (**no harmfull aliasing**)

→ the lowest possible sampling rate is in general given by

$$f_S \ge \frac{2f_C+B}{n_{\max}+1} = \frac{2f_C+B}{floor(\frac{2f_C-B}{2B})+1} = \frac{2f_C+B}{floor(\frac{2f_C-B}{2B}+1)} = \frac{2f_C+B}{floor(\frac{2f_C+B}{2B})}$$

- the "ultimate" sampling rate $f_S=2B$ is utilizable <u>iff</u> $\frac{2f_C+B}{2B}$ is an integer (then and only then $floor(\frac{2f_C+B}{2B}) = \frac{2f_C+B}{2B}$)

– **Numerical example:** $f_C = 20$ kHz and $B = 10$ kHz, so

→ $0 \le n \le floor(\frac{40-10}{20}) = floor(1.5) = 1$ and the possible values for f_S are

→ $n = 0$: $\quad 50 \text{ kHz} \le f_S \le \infty$

→ $n = 1$: $\quad 25 \text{ kHz} \le f_S \le 30 \text{ kHz}$

- try e.g. with $f_S = 27$ kHz and you see that no harmfull aliasing occurs

Complex subsampling

– Instead of sampling directly the real-valued signal, the idea is to sample the corresponding analytic signal !!!

– So the sampling structure looks like (HT denotes Hilbert transformer)

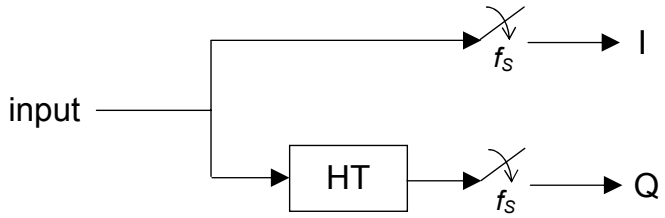

– Now since the analytic signal is free from negative frequency components, sampling frequency of $f_S = B$ (or any rate above) is always (independently of the center-frequency f_C !) sufficient to avoid harmfull aliasing !!!

– Some example spectral figures with the same input signal as in the previous subsection:

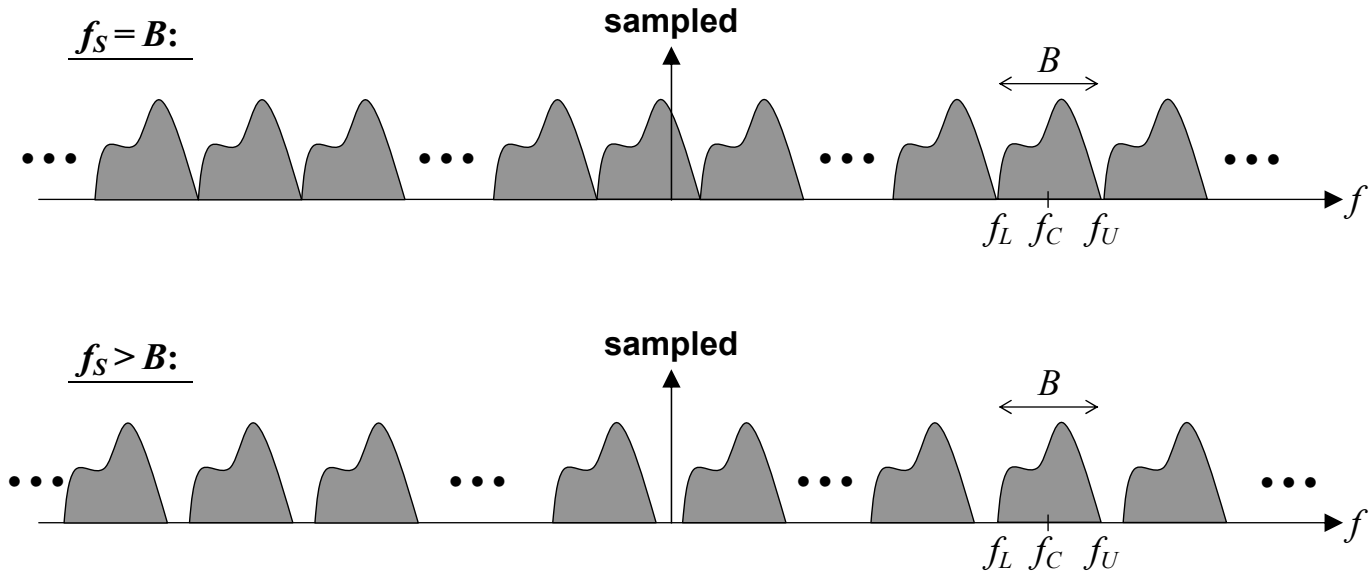

– **Notice:** If the center-frequency f_C is an integer multiple of the sample rate f_S (i.e., $f_S = f_C / k$), the center-frequency of the k-th spectral replica will coincide with zero frequency and a direct **bandpass-to-lowpass transformation** is obtained !!!

→ this is easy to understand based on spectral interpretations but can also be seen as follows:

- the real bandpass input, say $r(t)$, can be written in terms of its baseband equivalent $z(t)$ as

$$r(t) = \mathrm{Re}[z(t)e^{j\omega_C t}] = \frac{1}{2}z(t)e^{j\omega_C t} + \frac{1}{2}z^*(t)e^{-j\omega_C t}$$

- then the corresponding analytic signal is of the form

$$r(t) + jr_{HT}(t) = \frac{1}{2}z(t)e^{j\omega_C t} + \frac{1}{2}z^*(t)e^{-j\omega_C t} + j(-j\frac{1}{2}z(t)e^{j\omega_C t} + j\frac{1}{2}z^*(t)e^{-j\omega_C t})$$
$$= z(t)e^{j\omega_C t}$$

- thus sampling at $f_S = f_C / k$ (with k integer) results in

$$r(nT_S) + jr_{HT}(nT_S) = z(nT_S)e^{j\omega_C nT_S} = z(nT_S)e^{j2\pi f_C nT_S} = z(nT_S)e^{j2\pi nk} = z(nT_S)$$

which are indeed just the samples of the baseband equivalent

MULTIRATE PROCESSING OF BANDPASS AND I/Q SIGNALS

– The two fundamental multirate operations (**decimation/down-sampling** and **interpolation/up-sampling**) enable the sample rate to be altered digitally.

– In addition to this, they also offer an interesting alternative to mixing in performing frequency translations.

Decimation or Down-Sampling with Complex Signals

– The basic block-diagram to reduce the sample rate by an integer factor L is presented in the figure below, with f_S denoting the original sample rate.

– In the down-sampling ($\downarrow L$), every L-th sample of the input sequence is picked up to form the output sequence and the new sample rate becomes f_S/L.

– As a consequence, all the frequency bands located at the integer multiples of f_S/L (within $-f_S/2 \ldots f_S/2$ of course) are aliased down to baseband.

– These are also illustrated in the following figure.

– Thus, if the (generally complex) input signal is of lowpass type (passband $-B_{neg} \ldots B_{pos}$), the decimation filter $H(z)$ should attenuate all the frequency bands of width $B = B_{neg} + B_{pos}$ located correspondingly at the previous critical frequencies.

– Naturally, the bandwidth $B = B_{neg} + B_{pos}$ needs to be smaller than f_S/L
  → but there's no restriction such that, e.g., B_{pos} should be smaller than $(f_S/L)/2$
  → as long as $f_S/L \geq B$, the down-sampled signal is free from harmful aliasing
– On the other hand, if the desired signal is originally a bandpass signal (with a generally complex-valued baseband equivalent), the inherent aliasing can be exploited to change the signal center-frequency.
– Now, the decimation filter $H(z)$ is a bandpass filter selecting the desired frequency band, and aliasing can be used to bring the signal closer to baseband
  → as a special case of this, if the signal is **centered** at any multiple of the output sample frequency f_S/L, an analytic bandpass filter and decimation will result in a direct bandpass-to-lowpass transformation
  → this basically represents a digital equivalent of the complex (I/Q) subsampling scheme of the previous section
– Two example cases follow in the figures below.

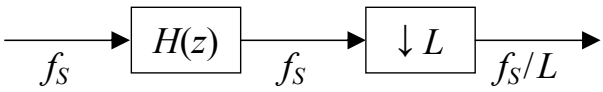

before down-sampling:

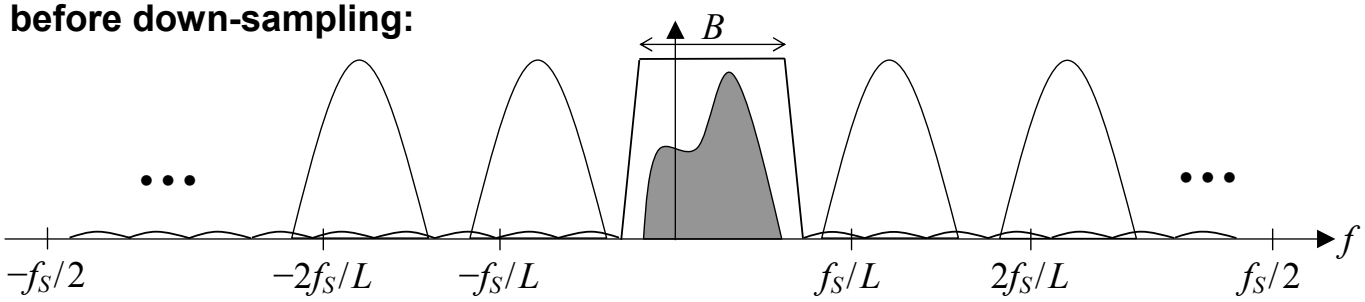

after down-sampling:

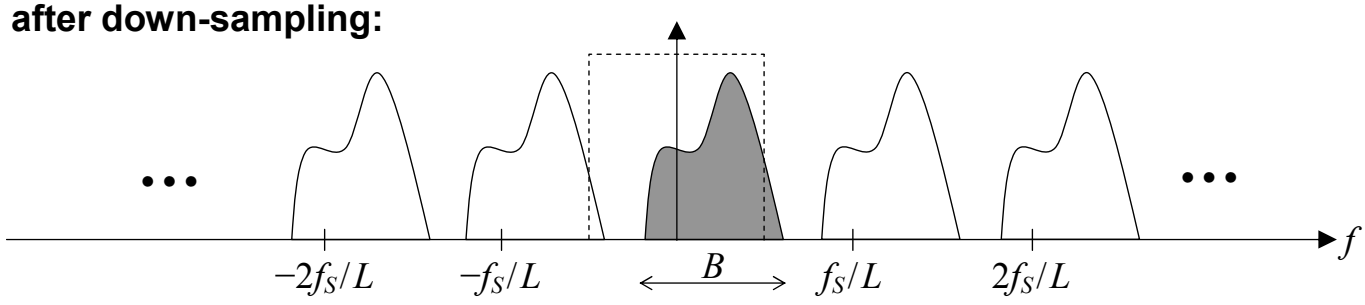

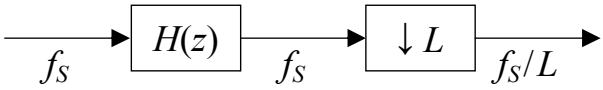

before down-sampling:

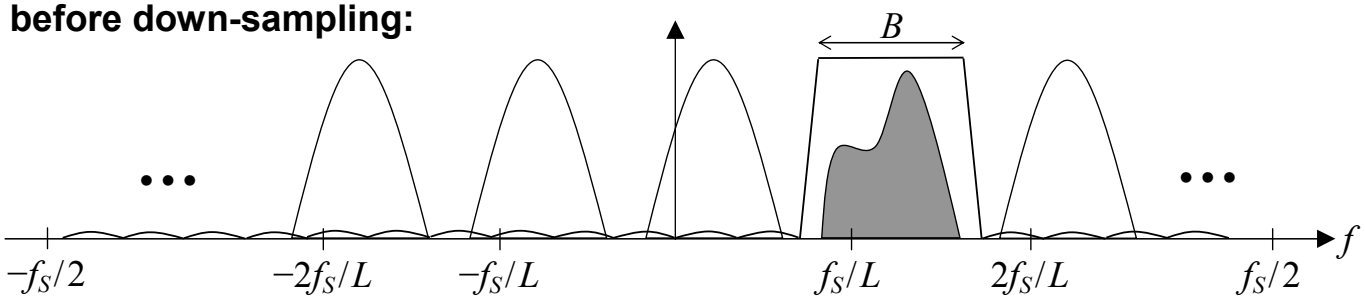

after down-sampling:

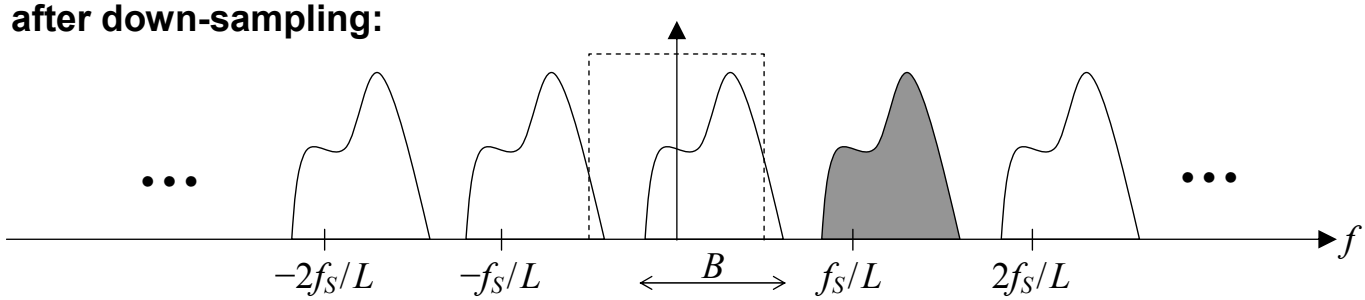

Interpolation or Up-Sampling with Complex Signals

- The basic block-diagram to increase the sample rate by an integer factor L is presented in the figure below, with f_S again denoting the original sample rate.
- The output sequence of the up-sampler ($\uparrow L$) is formed by adding $L-1$ zeros between each original input sample.
- As a consequence, all the spectral images (within $-Lf_S/2 \ldots Lf_S/2$) of the input spectrum appear now at the output signal at the multiples of the input sample rate f_S.
- These are illustrated in the following figure.
- Traditionally, the interpolation filter $H(z)$ attenuates these extra images retaining only the original spectral component.
- This is, however, not the only possibility. More precisely, any of the spectral images within $-Lf_S/2 \ldots Lf_S/2$ can be considered to be the desired one.
- As an example, the original lowpass signal can be transformed into a bandpass signal by simply using a proper bandpass filter as the interpolation filter $H(z)$. This filter now retains the spectral image at the desired center-frequency and attenuates the others.

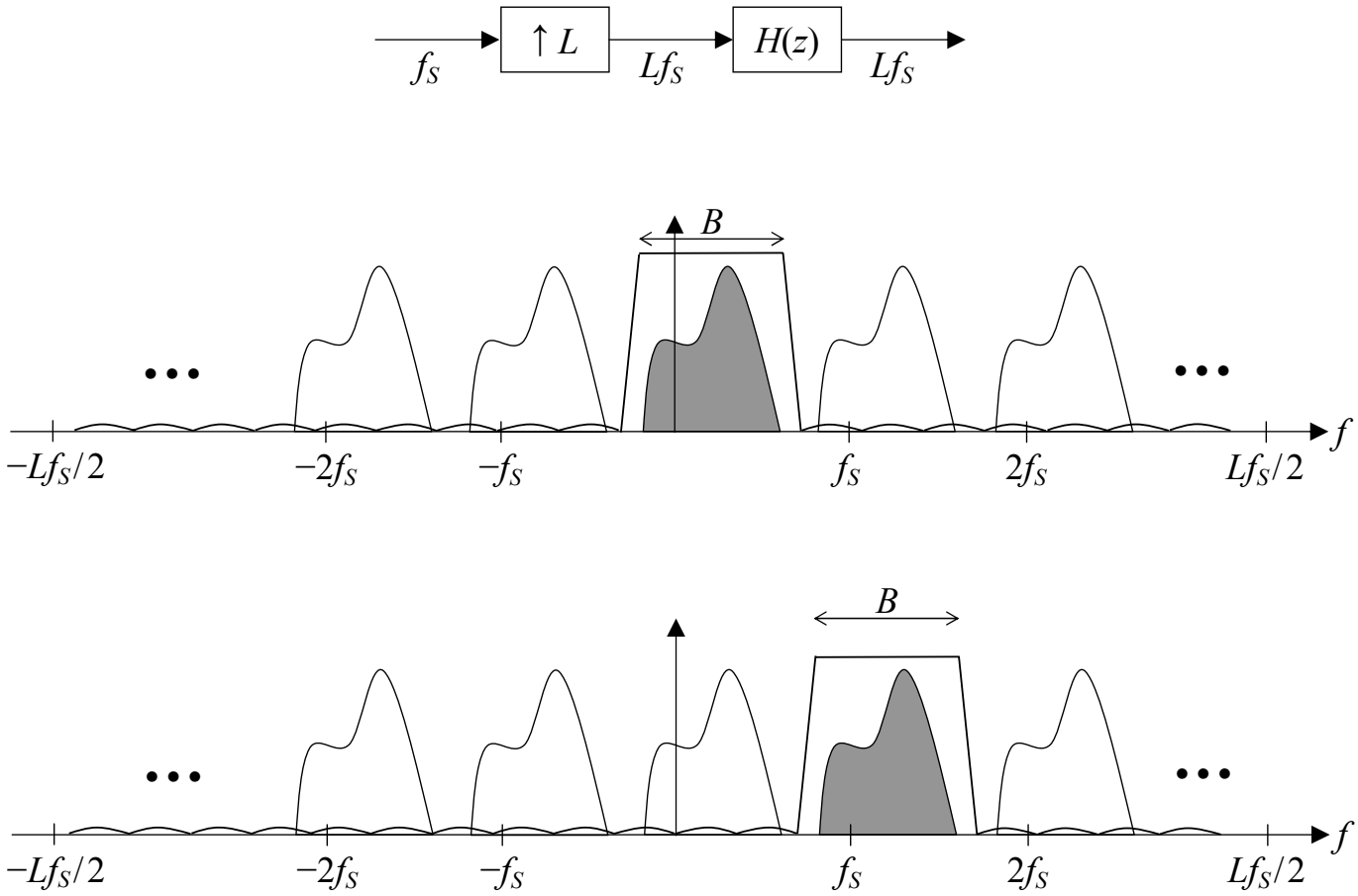

EFFICIENT POLYPHASE STRUCTURES

- Polyphase filtering represents one interesting approach to implement decimation or interpolation in a flexible yet computationally efficient way.
- In the traditional approaches, the decimation/interpolation filters operate at the **higher sampling rate**, i.e., either before down-sampling or after up-sampling.
- Given that the down-/up-sampling ratio is L, the idea in the polyphase structures is to split the related filtering into L parallel stages operating at the **lower sampling rate**

  → in applications requiring very high operation speeds, this can be a crucial benefit
- Furthermore, the polyphase structures are quite flexible if used, e.g., in channelization applications.
- These aspects will be explained in more detail in the following.

Polyphase Decomposition of FIR filters

– The so called polyphase decomposition of a finite length filter $H(z)$ is usually formulated as

$$H(z) = \sum_{i=0}^{L-1} z^{-i} H_i(z^L)$$

– To put it in words, the output of any FIR filter in general can be constructed as a sum of the outputs of the filters $H_0(z^L)$, $H_1(z^L)$, …, $H_{L-1}(z^L)$ whose input signals are delayed by z^0, z^{-1}, …, $z^{-(L-1)}$.

– Given that the impulse response of $H(z)$ is $h(n)$, the impulse responses of $H_0(z)$, $H_1(z)$, …, $H_{L-1}(z)$ are simply

$$h_0(n) = \{h(0), h(L), ...\}$$
$$h_1(n) = \{h(1), h(L+1), ...\}$$
$$\vdots$$
$$h_{L-1}(n) = \{h(L-1), h(2L-1), ...\}$$

– **Example:** Two-phase decomposition of $H(z)=h(0)+h(1)z^{-1}+\ldots+h(14)z^{-14}$ is

$$\begin{aligned} H(z) &= h(0)+h(2)z^{-2}+h(4)z^{-4}+h(6)z^{-6}+h(8)z^{-8}+h(10)z^{-10}+h(12)z^{-12}+h(14)z^{-14} \\ &\quad + z^{-1}(h(1)+h(3)z^{-2}+h(5)z^{-4}+h(7)z^{-6}+h(9)z^{-8}+h(11)z^{-10}+h(13)z^{-12}) \\ &= H_0(z^2)+z^{-1}H_1(z^2) \end{aligned}$$

where

$h_0(n)=\{h(0), h(2), h(4), h(6), h(8), h(10), h(12), h(14)\}$

$h_1(n)=\{h(1), h(3), h(5), h(7), h(9), h(11), h(13)\}$

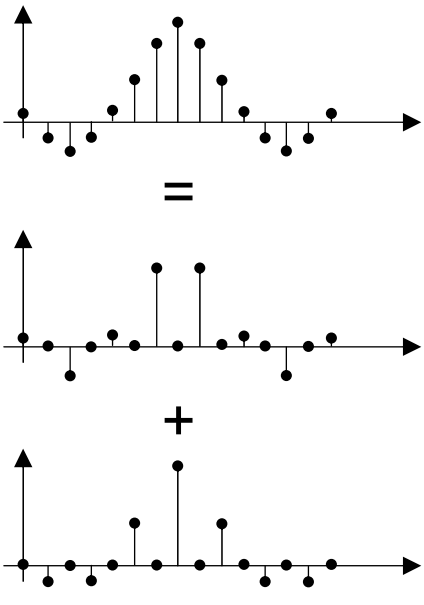

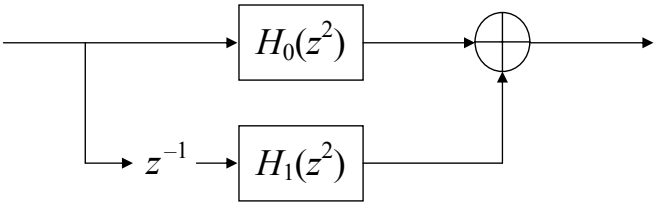

Basic Polyphase Decimators and Interpolators

- In **decimation** applications, the down-sampler which traditionally operates on the filter output can now be transferred to the front of the branch filters given that the L time delays in the filters $H_0(z^L)$, …, $H_{L-1}(z^L)$ are replaced by ordinary unit delays
  → this operation is intuitively clear and theoretically justified by the famous **noble identity** of multirate signal processing
- So in the *i*-th branch, the input signal is delayed by z^{-i}, down-sampled by L, and filtered using $H_i(z)$.
- Finally, the outputs of the L branches are summed to form the final decimated output signal.
- Notice that all the branch filters operate at the lower sampling rate !
- This is illustrated in the following using a simple example.

- **Example (cont'd):** Down-sampling by $L=2$.

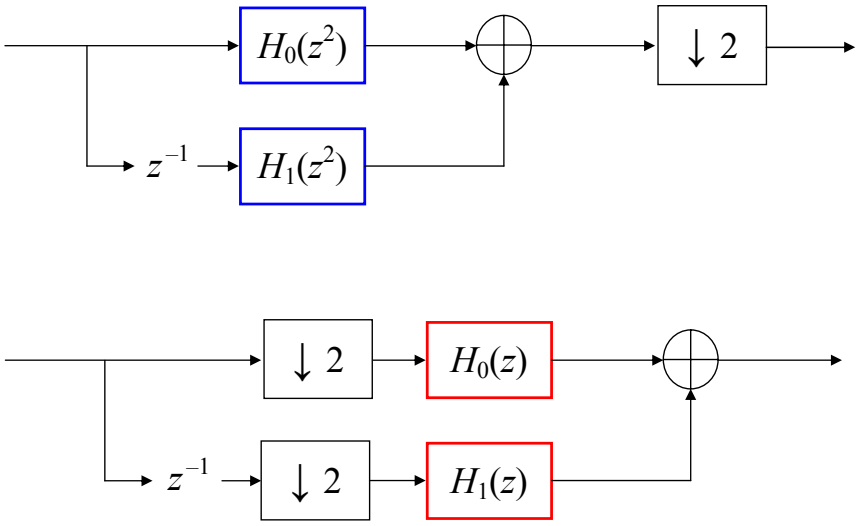

- Since in general the delay z^{-i} is different in every branch and the down-samplers operate synchronously, the low-rate data sequences entering the branch filters are all disjoint.

– Thus, the front-end delays and down-samplers can actually be discarded by simply feeding every L-th (with a proper time-shift) sample to the polyphase branches using a commutative switch.

– This final structure is depicted in the figure below.

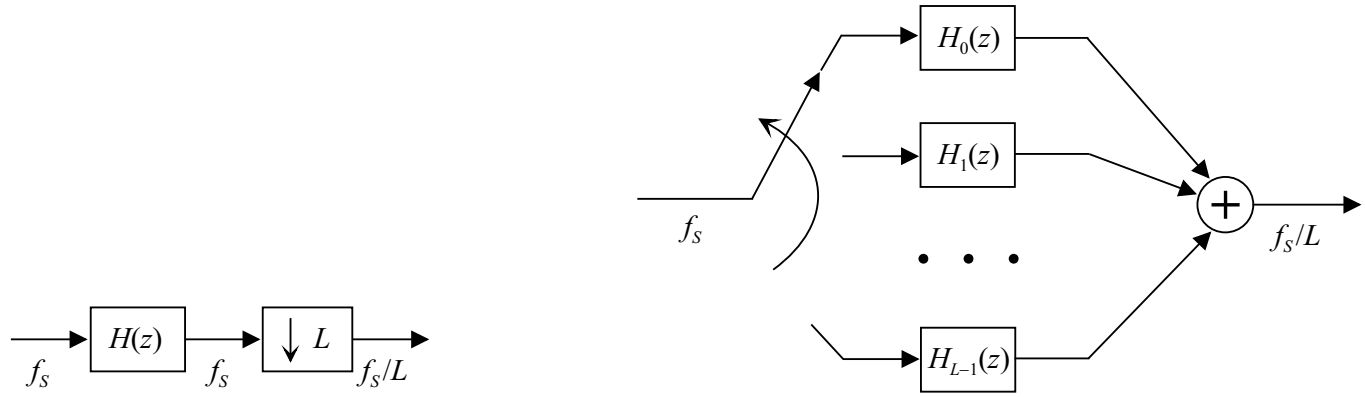

Figure. (a) The basic decimation (down-sampling) scheme. (b) The corresponding polyphase implementation.

– Similar reasoning can be used also in the **interpolation** case.

– The traditional approach based on zero-padding and filtering maps into a polyphase structure where the input signal to be interpolated is fed directly into the branch filters $H_0(z)$, $H_1(z)$, …, $H_{L-1}(z)$.

– The outputs of these filters are then up-sampled and delayed, the delay being z^{-i} in the *i*-th branch, and finally summed to form the interpolator output.

– Due to zero-packing and different branch delays, only one branch filter output actually contributes to the final output (with other outputs being zero) at any given time instant.

– Thus, as in the decimation case, the final structure can be implemented by simply multiplexing the branch filter outputs using a commutator.

– This approach is pictured below.

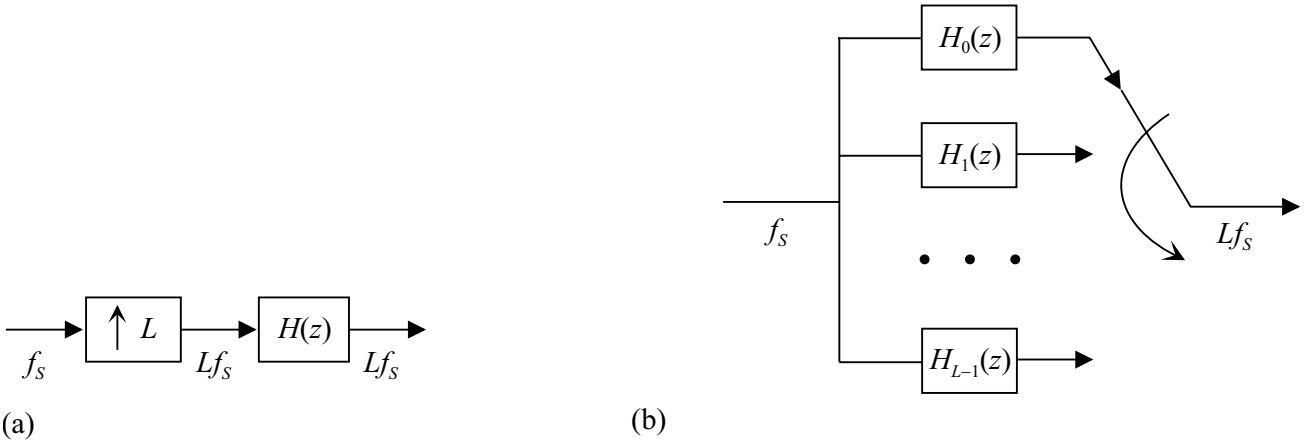

Figure. (a) The basic interpolation (up-sampling) scheme. (b) The corresponding polyphase implementation.

- One interesting interpretation of the previous polyphase structures is related to **aliasing** and the **amplitude and phase characteristics** of the polyphase filters.
- As an example, consider the decimation case. Since the input signal is directly down-sampled in each polyphase branch, all the bands located at the integer multiples of the final output sampling rate alias to baseband.
- However, due to the relative delays of the different branches as well as different phase characteristics of the polyphase filters, only the information within the passband of the prototype filter $H(z)$ will appear in the final decimator output.
- To be more specific, all the polyphase branch filters are actually **allpass filters** whose amplitude response is ideally constant.
- Furthermore, the phase delays of the different filters differ by $1/L$ with $H_0(z)$ having the largest delay.
- This is easy to see even intuitively when considering how the polyphase filters are obtained from the "prototype" $H(z)$.

Bandpass Polyphase Structures

- The previous discussion is basically valid for both **lowpass** and **bandpass** decimator/interpolator structures.
- The only difference is, of course, related to the characteristics and design of the filter $H(z)$.
- A straight-forward way to handle the lowpass and bandpass cases is to consider them separately.
- However, the full flexibility of the polyphase structures can only be capitalized by treating them together.
- To illustrate the basic idea, assume the filter $H(z)$ is designed for a specific lowpass decimation scenario (passband $-B_{neg} \ldots B_{pos}$ in general).
- Now, suppose we wish to change the structure to process a bandpass signal located around a center-frequency f_C which is an **integer multiple of the output rate** f_S/L.
- In terms of the normalized frequency variable $\omega = 2\pi f/f_S$, this means that ω_C is an integer multiple of $2\pi/L$.

- In general, an analytic filter $G(z)$ to extract the interesting band can be obtained simply by frequency translating the corresponding lowpass prototype filter $H(z)$ as $g(n) = h(n)\exp\{j\omega_C n\}$.
- The impulse responses of the corresponding polyphase implementation of $g(n)$ are then obtained as presented before, i.e., $g_0(n) = \{g(0), g(L), \ldots\}$, $g_1(n) = \{g(1), g(L+1), \ldots\}$, etc.
- However, after some manipulations, the polyphase impulse responses for the analytic filter $G(z)$ can simply be written as

$$
\begin{aligned}
g_0(n) &= h_0(n) \\
g_1(n) &= h_1(n) \times \exp\{jk(2\pi)/L\} \\
g_2(n) &= h_2(n) \times \exp\{jk(2\pi)2/L\} \\
&\vdots \\
g_{L-1}(n) &= h_{L-1}(n) \times \exp\{jk(2\pi)(L-1)/L\}
\end{aligned}
$$

  where the integer k is the "channel index", i.e., $\omega_C = k(2\pi/L)$.

  => the same polyphase representation as in the lowpass case except for the constant complex multipliers $\exp(jk(2\pi)i/L)$!!!

– **Example:** Bandpass down-sampling by $L=4$ with $\omega_C=\pi/2$ (i.e., $f_C=f_S/4$),

$g(n)=h(n)\exp(j(\pi/2)n)$

$$g_0(n)=\{h(0)e^{j\frac{\pi}{2}0}, h(4)e^{j\frac{\pi}{2}4}, h(8)e^{j\frac{\pi}{2}8}, ...\}=\{h(0), h(4), h(8), ...\}$$

$$g_1(n)=\{h(1)e^{j\frac{\pi}{2}1}, h(5)e^{j\frac{\pi}{2}5}, h(9)e^{j\frac{\pi}{2}9}, ...\}=\{h(1), h(5), h(9), ...\}e^{j\frac{\pi}{2}}$$

$$g_2(n)=\{h(2)e^{j\frac{\pi}{2}2}, h(6)e^{j\frac{\pi}{2}6}, h(10)e^{j\frac{\pi}{2}10}, ...\}=\{h(2), h(6), h(10), ...\}e^{j\pi}$$

$$g_3(n)=\{h(3)e^{j\frac{\pi}{2}3}, h(7)e^{j\frac{\pi}{2}7}, h(11)e^{j\frac{\pi}{2}11}, ...\}=\{h(3), h(7), h(11), ...\}e^{j\frac{3\pi}{2}}$$

– So as stated before, the modulating exponentials in the polyphase filters reduce to constant multipliers $w_{i,k}=\exp\{jk(2\pi)i/L\}$, $i=1, 2, \ldots, L-1$.

– This effect, in turn, can be implemented by simply multiplying the outputs of the **lowpass** polyphase filters by the constants $w_{i,k}$!!!

– As a consequence, the same polyphase front-end (the same filters !!!) can be used to extract any channel located at the multiple of the output rate.

– This general polyphase decimator structure is illustrated in the figure below.

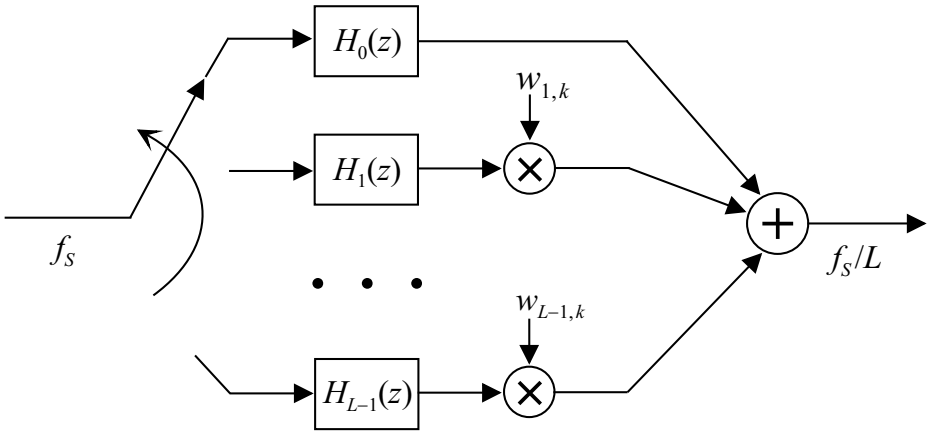

Figure. General polyphase decimator.

– Similar type reasoning can again be used also in the interpolation (up-sampling) case.

Matlab Demo

- The previous ideas of bandpass polyphase filtering and decimation are illustrated using Matlab.
- As an example case, we have three channels
  - → #1: $\omega_{C1} = 0.25\pi$, 8PSK modulated signal, 16 samples per symbol
  - → #2: $\omega_{C2} = 0.50\pi$, 4PSK modulated signal, 16 samples per symbol
  - → #3: $\omega_{C3} = 0.75\pi$, 16QAM modulated signal, 16 samples per symbol
- In all the cases, raised-cosine pulse-shape with 35% roll-off is used.
- Since the channels are centered at integer multiples of $\pi/4$ (i.e., $f_S/8$), we use a polyphase structure with L=8
  - → after downsampling and polyphase filtering, a further decimation by 2 is included to get symbol rate samples (in order to plot the output constellations)
- The simulation setup and the results are illustrated in the following figures.

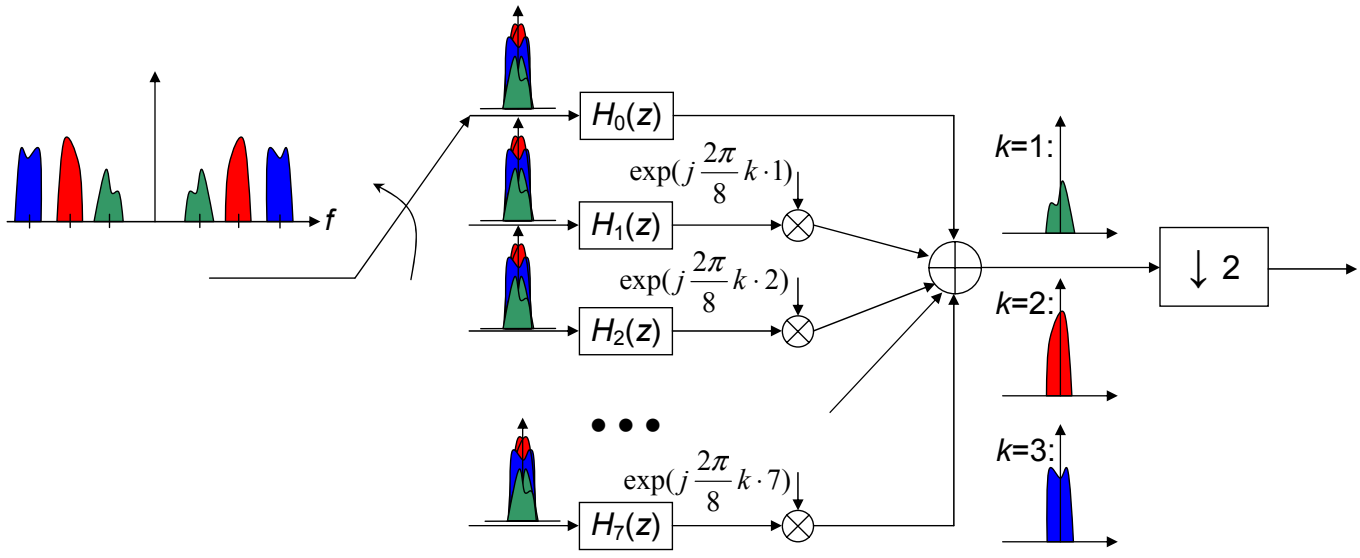

Figure. Demonstration set-up, $L = 8$.

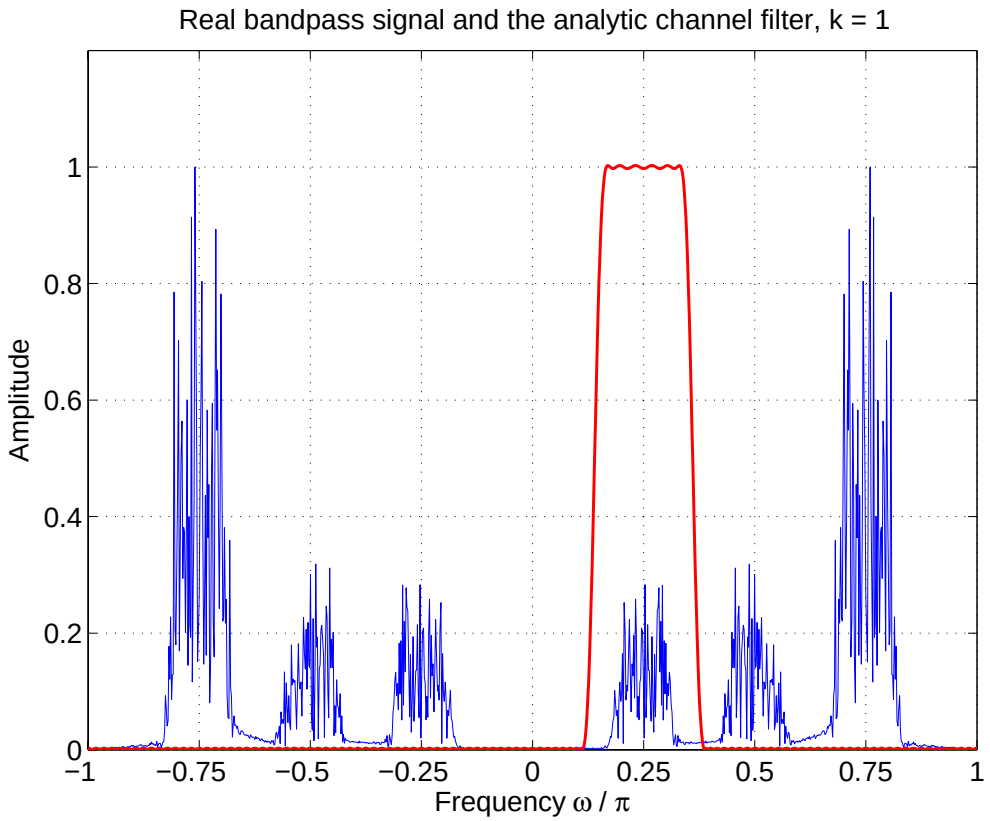

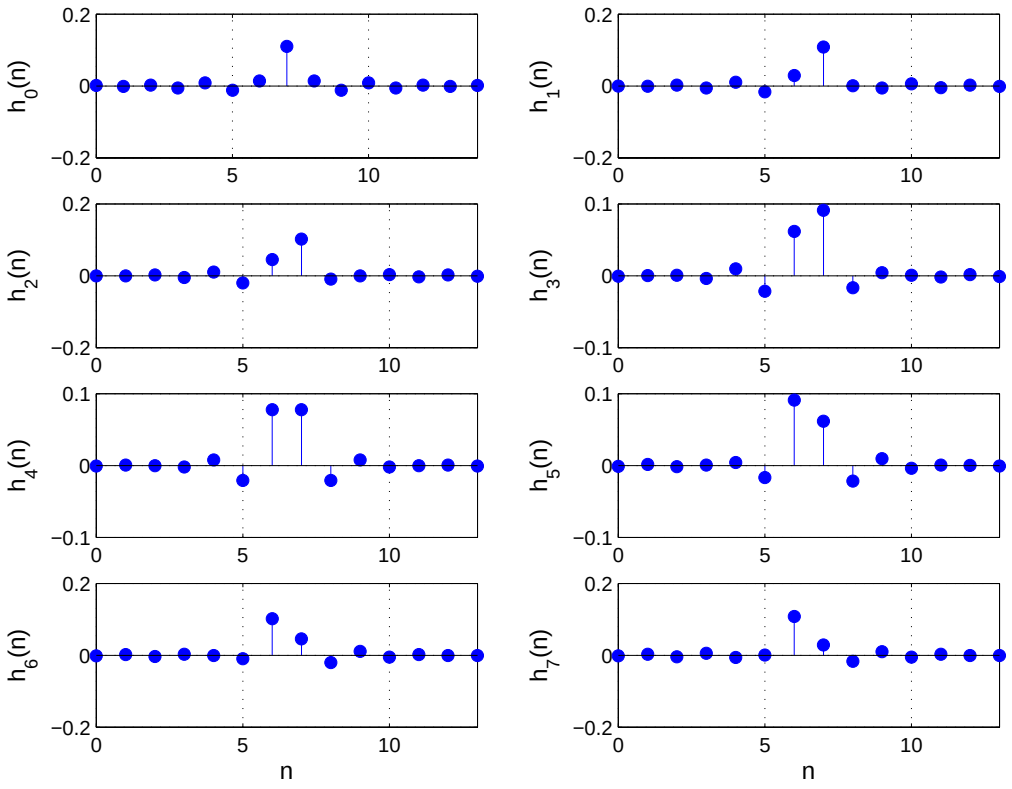

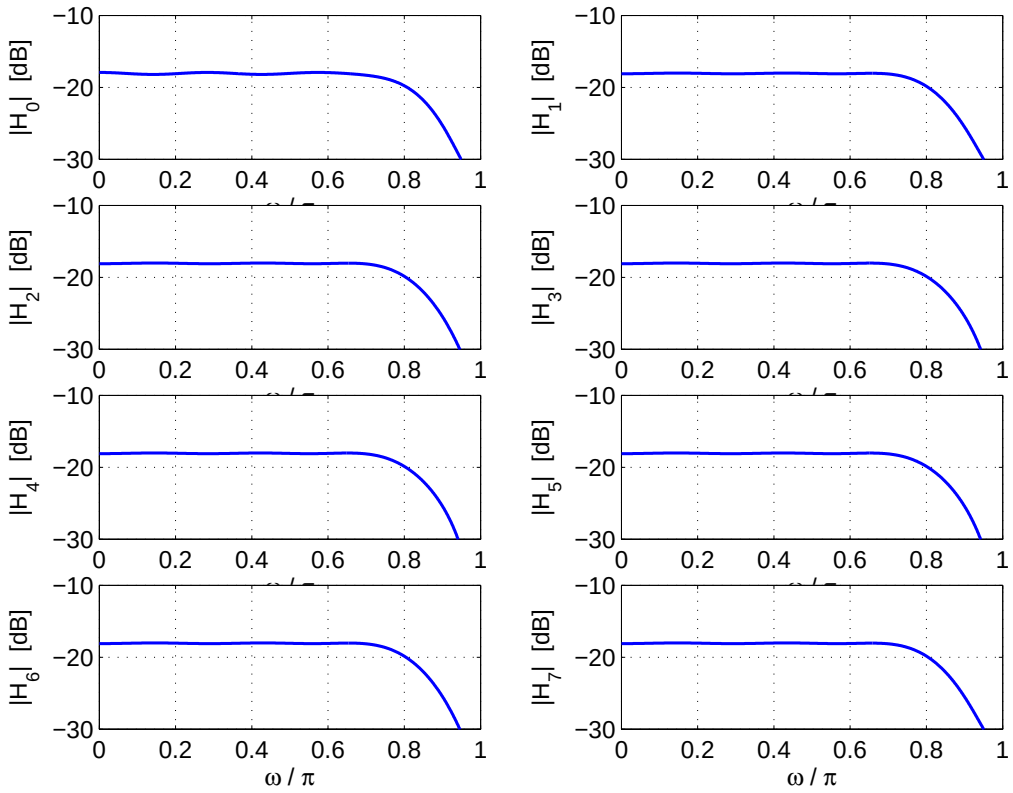

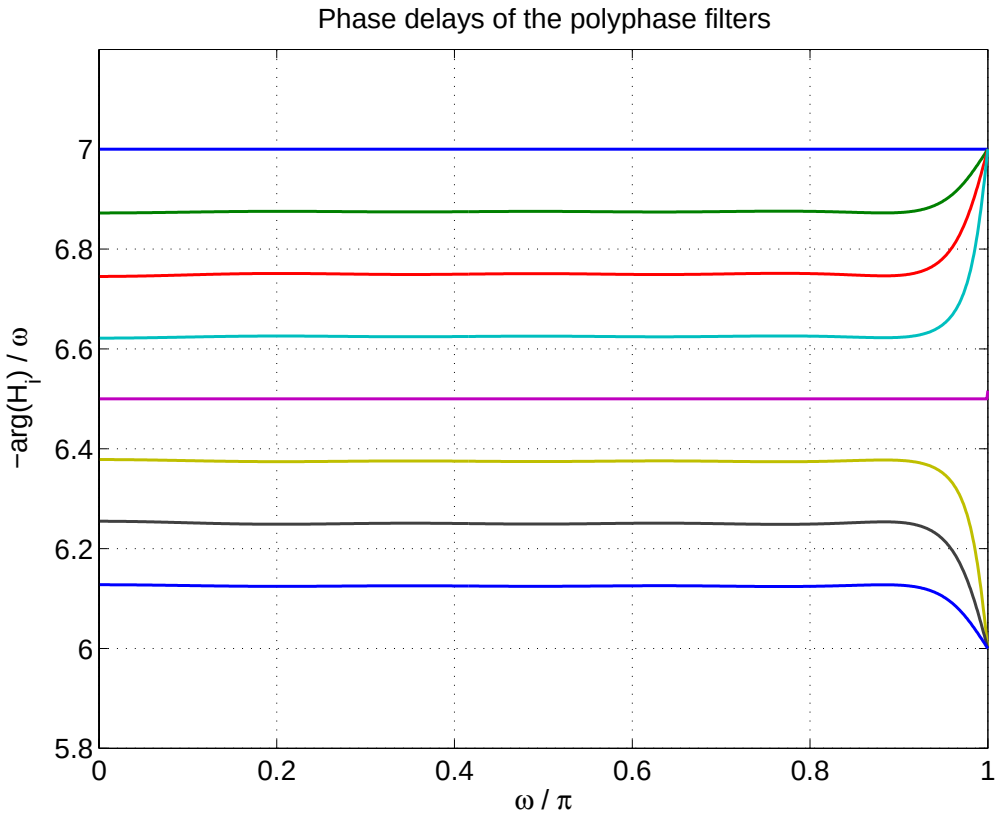

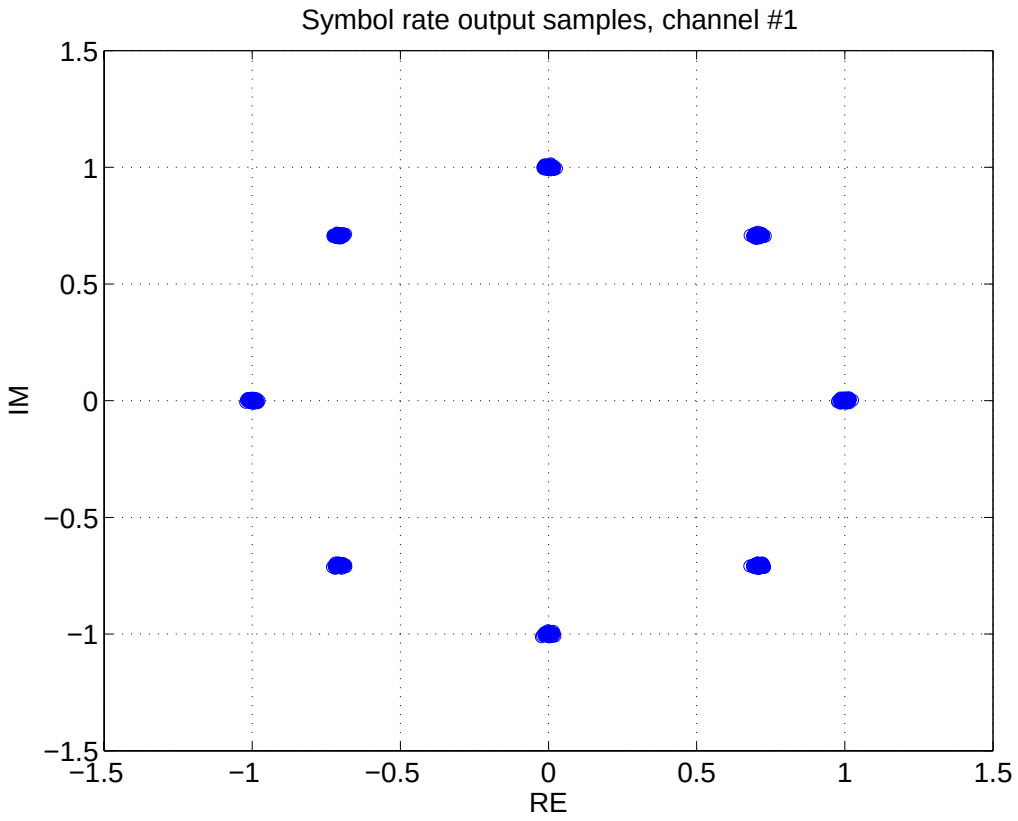

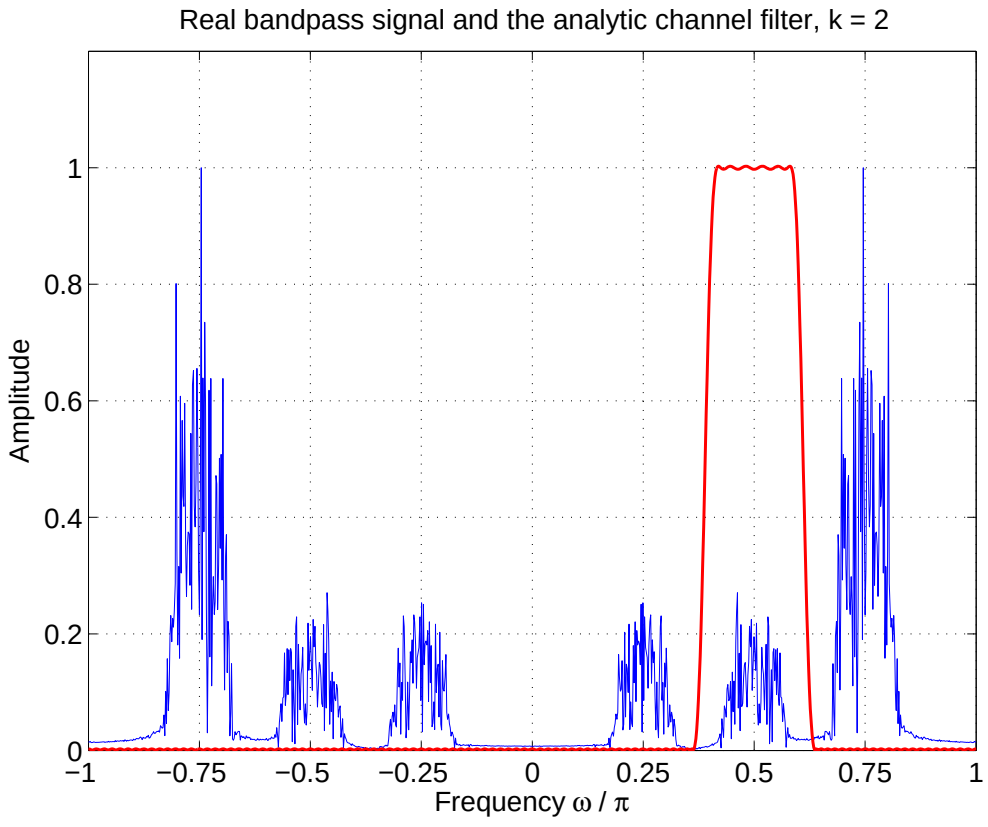

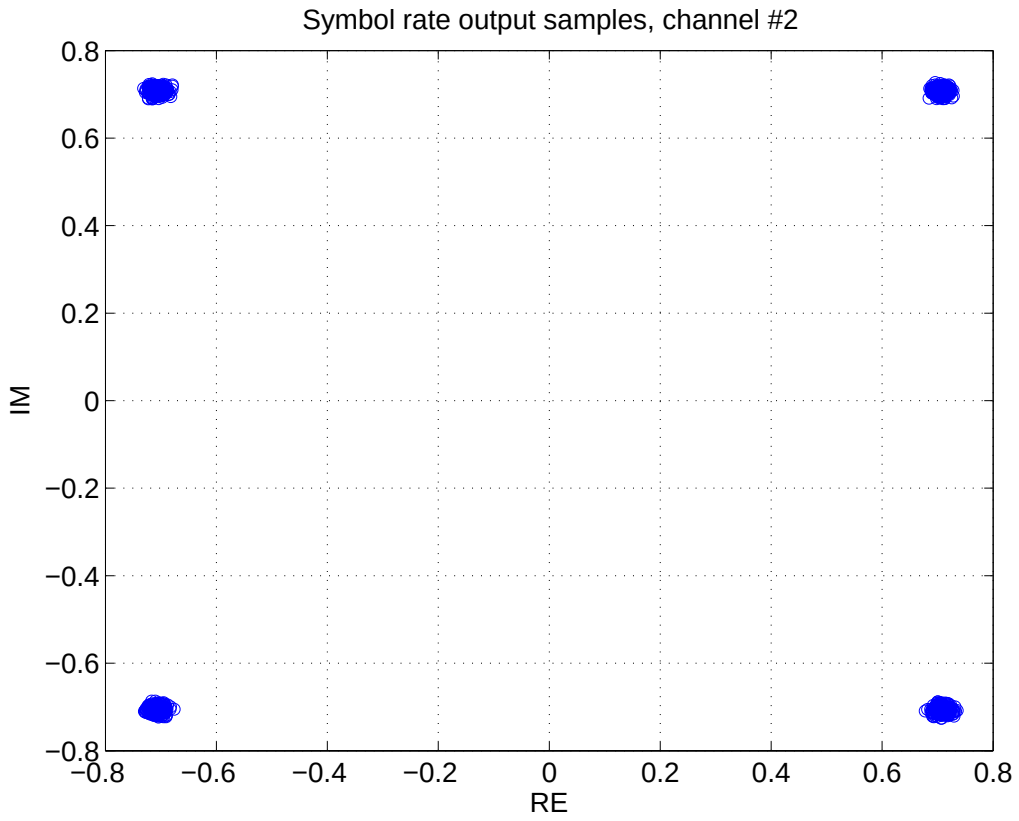

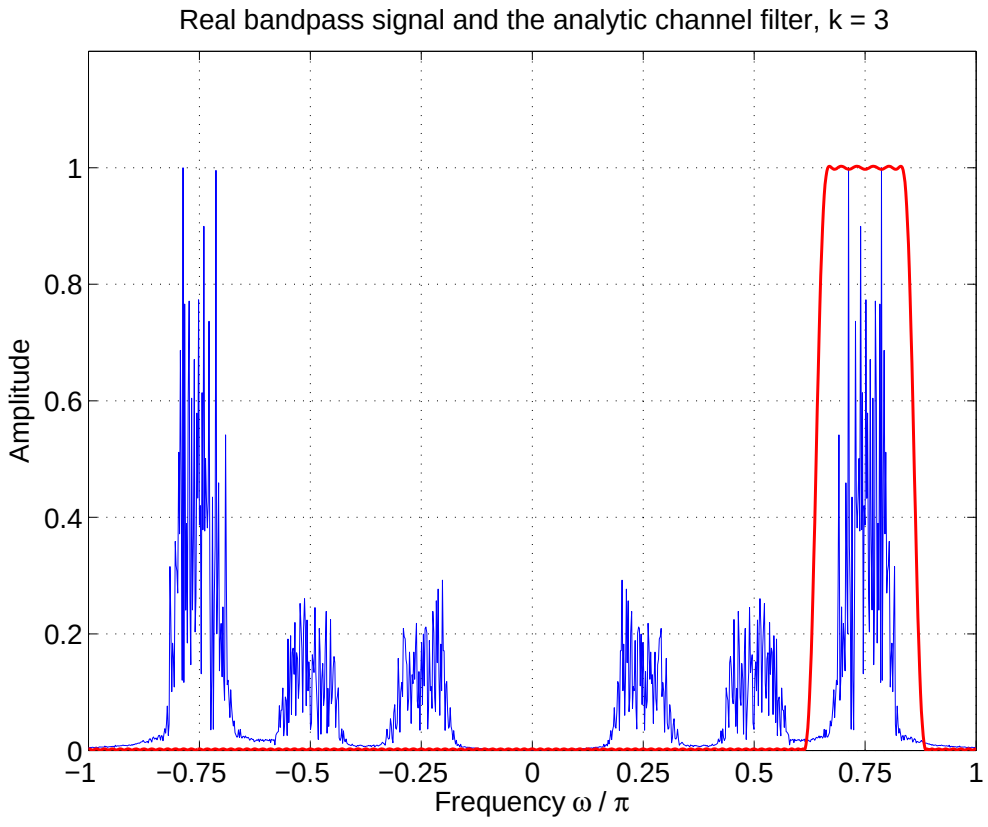

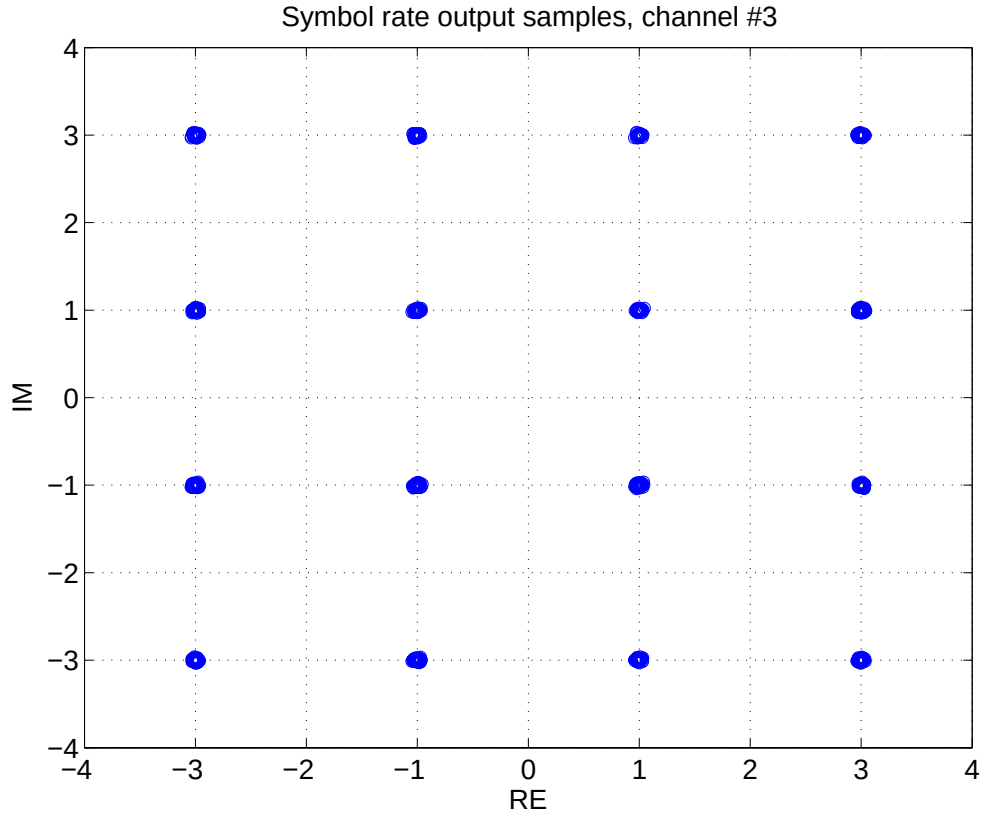

- Notice that even though analytic channel filters are shown in the three figures, the actual implementation is really based on the polyphase concepts.
- In other words, there is no single filter with the given response but the polyphase decimator effectively implements that kind of function.
- Remember also that the branch filters for each channel (k = 1, 2, 3) are identical, only the "scaling" coefficients $w_{i,k}$ after the filters depend on the channel index.
- Notice also that **the structure works similarly for complex input signals** as well (in the previous example, the input is real-valued).

3. I/Q Mismatch Problems in Analog I/Q Signal Processing

I/Q Signal Processing in Receivers

– In communication receivers, one of the key front-end functionalities is to **down-convert the desired channel signal from RF closer to baseband, in the presence of other channels/signals**.

– In this context, **the fundamental problem of image signal attenuation** is a major concern.

– Traditionally, in superheterodyne (and its variants) receivers, the image band is attenuated using RF filtering before the down-conversion stage

→ the basic image signal problem is illustrated in the following figure where the target is to translate the desired channel signal to an intermediate frequency (IF) f_{IF}

- the desired channel is illustrated in grey and it's image in dark, separated in frequency by $2f_{IF}$

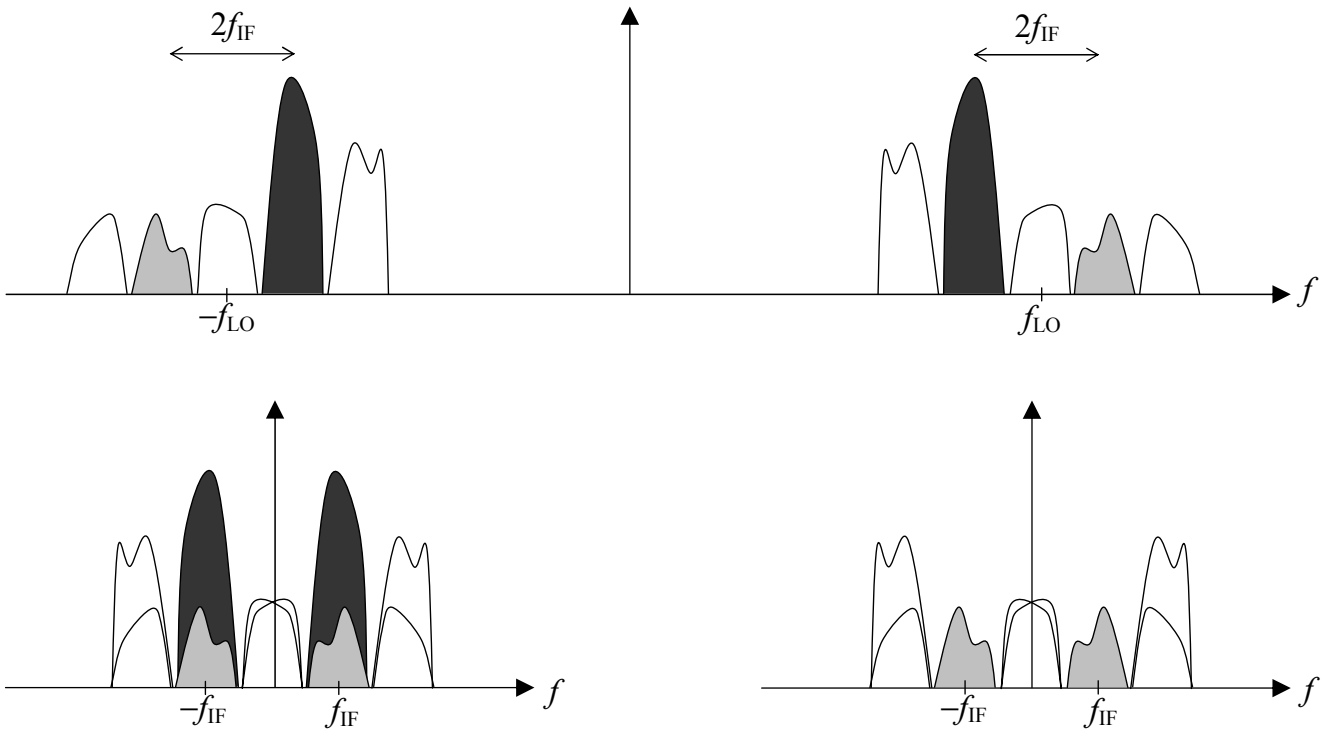

– The lower part illustrates the signal after down-conversion and lowpass filtering without (left) and with (right) RF image rejection filtering.

– In practice a tradeoff is needed in the selection of the IF:
  → the higher the IF, the easier it is to implement the RF image rejection filter (since the separation of the desired and image bands is $2f_{IF}$)
  → on the other hand, the lower the IF, the easier it is to implement the channel selectivity filtering
– **In order to reduce the needed RF image rejection filtering, complex (I/Q) down-conversion can be used instead of real mixing**
  → theoretically a pure frequency translation and image problems are avoided during the frequency shift
  → this idea can be used in the receiver front-end simply for down-conversion purposes, independently of the desired channel modulation
– A generalized receiver based on this idea appears in figure below.
– The **90° phase shift** can basically be introduced either between the local oscillator (LO) signals (point A) or between the input signal branches (point B)
  → **point A:** $\cos(.)$ and $-\sin(.)$ LO signals
  → **point B:** a wideband Hilbert transformer (and two in-phase LOs)

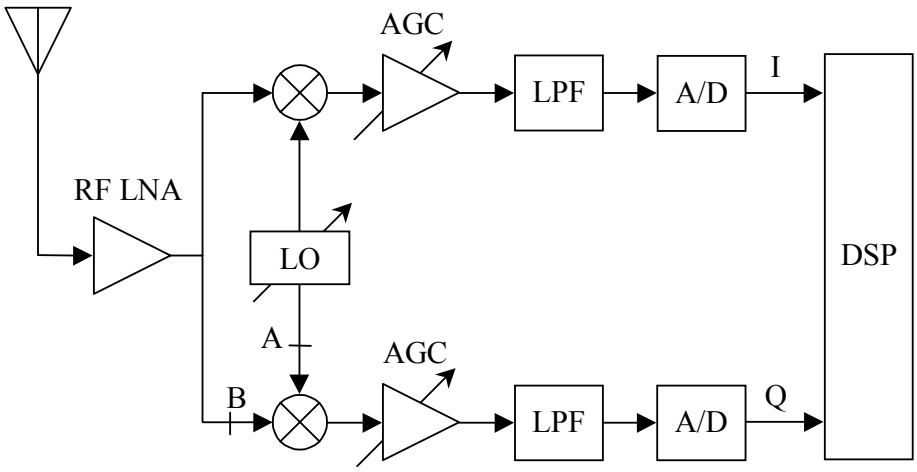

– **In theory:** the resulting I and Q channels should have equal amplitudes and a phase difference of $90°$
  → **infinite attenuation for the image signal band**
– **In practice:** real-world analog components, such as the mixers, LPFs, etc., can never be perfectly matched
  → **some imbalance will always exist**
  → **the image attenuation is finite** (formal proof will be given later)

– 1-2° and 1-2% imbalance values are realistic, resulting in **20-40 dB image attenuation**.

– To be more precise, let's start to look at the **following situation in more detail:**

→ wideband front-end, no image rejection filtering (idealized case)

→ multichannel (see the following figure) bandpass signal (bandwidth B) centered at f_{LO}

→ **target:** produce a wideband baseband equivalent of the received signal (wideband downconversion)

→ **how:** using I/Q signal processing

– **Obtain a formal characterization of the imbalance effects due to the mismatches of practical analog electronics**

→ first some basic results are given in the case when the amplitudes and/or phases of the two components (I and Q) of a complex signal become mismatched

→ these results are then applied to the wideband receiver case

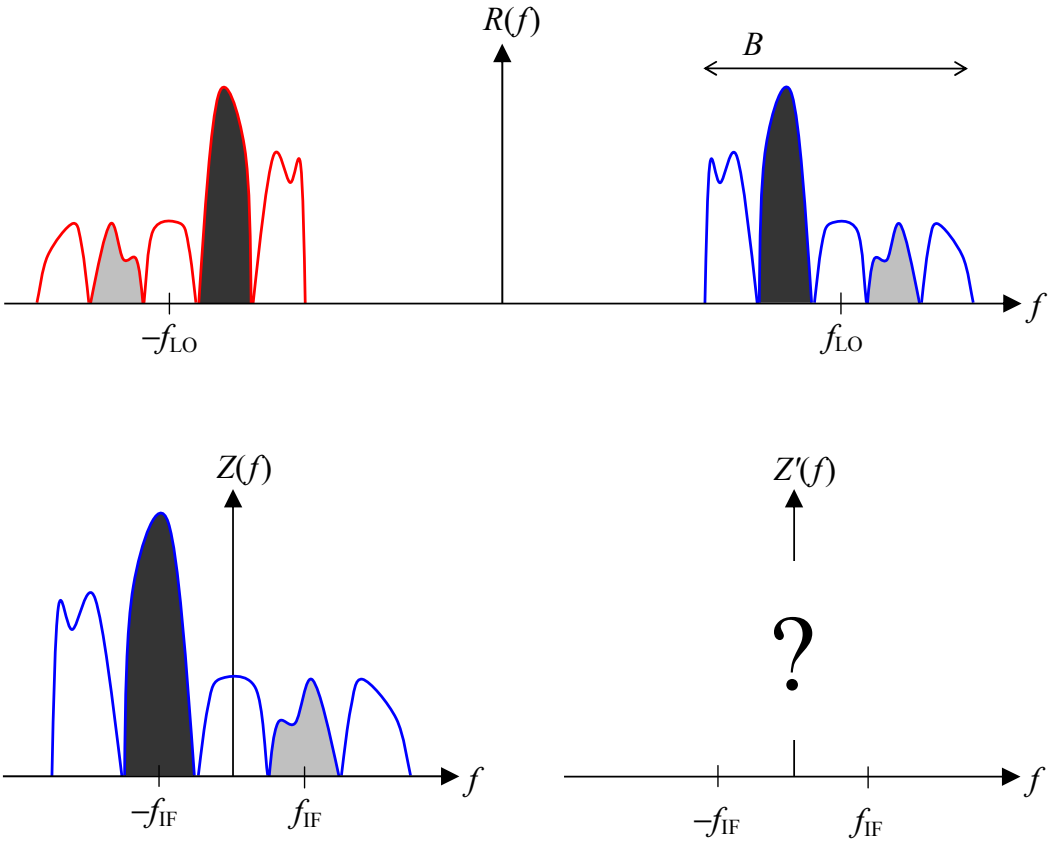

Narrowband Imbalance Model

- Consider an **ideal single frequency signal** $z(t) = e^{j\omega_0 t} = \cos(\omega_0 t) + j\sin(\omega_0 t)$.
- Here, we assume that the mismatched I and Q components have
  → relative amplitudes g_1 and g_2
  → relative phases ϕ_1 and ϕ_2
- In other words, we write the **imbalanced signal** $z'(t)$ as

$$z'(t) = g_1 \cos(\omega_0 t + \phi_1) + j g_2 \sin(\omega_0 t + \phi_2)$$

- **Recap:** Euler's formulas $\cos(x) = \frac{e^{jx} + e^{-jx}}{2}$ and $\sin(x) = \frac{e^{jx} - e^{-jx}}{2j}$.
- Then, using the Euler's formulas, $z'(t)$ can be written as

$$z'(t) = \left(\frac{g_1 e^{j\phi_1} + g_2 e^{j\phi_2}}{2} \right) e^{j\omega_0 t} + \left(\frac{g_1 e^{-j\phi_1} - g_2 e^{-j\phi_2}}{2} \right) e^{-j\omega_0 t}$$

- So, in addition to the original component $e^{j\omega_0 t}$, $z'(t)$ consists also of the **mirror frequency component** $e^{-j\omega_0 t}$.
- Considering the **relative strengths of the two frequency components**, $z'(t)$ can also be written as

$$z'(t) = \left(\frac{1 + \frac{g_2}{g_1} e^{j(\phi_2 - \phi_1)}}{2} \right) g_1 e^{j\phi_1} e^{j\omega_0 t} + \left(\frac{1 - \frac{g_2}{g_1} e^{-j(\phi_2 - \phi_1)}}{2} \right) g_1 e^{-j\phi_1} e^{-j\omega_0 t}$$

$$= \left(\frac{1 + \frac{g_2}{g_1} e^{j(\phi_2 - \phi_1)}}{2} \right) g_1 e^{j(\omega_0 t + \phi_1)} + \left(\frac{1 - \frac{g_2}{g_1} e^{-j(\phi_2 - \phi_1)}}{2} \right) g_1 e^{-j(\omega_0 t + \phi_1)}$$

- So we notice that the relative strengths of the two frequency components depend only on the ***relative* amplitude and phase imbalances**
  → g_2 / g_1 and $\phi_2 - \phi_1$

– Therefore, to simplify the notations, we assume
  → $g_1 = 1$, $g_2 = g$ and
  → $\phi_1 = 0$, $\phi_2 = \phi$
– Then, the model can be written in a more simple form as

$$z'(t) = \left(\frac{1 + ge^{j\phi}}{2}\right)e^{j\omega_0 t} + \left(\frac{1 - ge^{-j\phi}}{2}\right)e^{-j\omega_0 t}$$

Wideband Imbalance Model

– ***Theorem:*** Consider a complex-valued signal $z(t) = z_I(t) + jz_Q(t)$ and its complex conjugate $z^*(t) = z_I(t) - jz_Q(t)$ whose **Fourier transforms** are given by
  → $z(t) \Leftrightarrow Z(f) = Z_I(f) + jZ_Q(f)$
  → $z^*(t) \Leftrightarrow Z^*(-f) = Z_I^*(-f) - jZ_Q^*(-f) = Z_I(f) - jZ_Q(f)$

  Then, the Fourier transform of $Z'(f) = H_I(f)Z_I(f) + jH_Q(f)Z_Q(f)$ can be written as

$$Z'(f) = \left(\frac{H_I(f) + H_Q(f)}{2}\right)Z(f) + \left(\frac{H_I(f) - H_Q(f)}{2}\right)Z^*(-f)$$

– ***Proof:*** Direct substitution (next page) will yield

$$\begin{aligned}
Z'(f) &= \left(\frac{H_I(f) + H_Q(f)}{2}\right)Z(f) + \left(\frac{H_I(f) - H_Q(f)}{2}\right)Z^*(-f) \\
&= \left(\frac{H_I(f) + H_Q(f)}{2}\right)\left(Z_I(f) + jZ_Q(f)\right) + \left(\frac{H_I(f) - H_Q(f)}{2}\right)\left(Z_I(f) - jZ_Q(f)\right) \\
&= \left(\frac{H_I(f)Z_I(f) + jH_I(f)Z_Q(f) + H_Q(f)Z_I(f) + jH_Q(f)Z_Q(f)}{2}\right) \\
&\quad + \left(\frac{H_I(f)Z_I(f) - jH_I(f)Z_Q(f) - H_Q(f)Z_I(f) + jH_Q(f)Z_Q(f)}{2}\right) \\
&= H_I(f)Z_I(f) + jH_Q(f)Z_Q(f) \quad \text{q.e.d.}
\end{aligned}$$

– As can be observed, the **mismatches cause a signal component relative to** $z^*(t)$ to appear in addition to the original signal component $z(t)$!

– Again, only the difference between $H_I(f)$ and $H_Q(f)$ contribute to the relative strength of the **mirror component** $Z^*(-f)$ (i.e., $z^*(t)$).

– Clearly, **a generalization of the narrowband case**.

Imbalance Effects in Receiver Front-Ends

– In general, all the analog components such as the
→ **quadrature mixing stage**
→ **branch filters**
→ **A/D converters**
affecting the I and Q branch signals contribute to the effective amplitude and phase mismatches.

– Motivated by this, the model of the following figure is used hereafter.

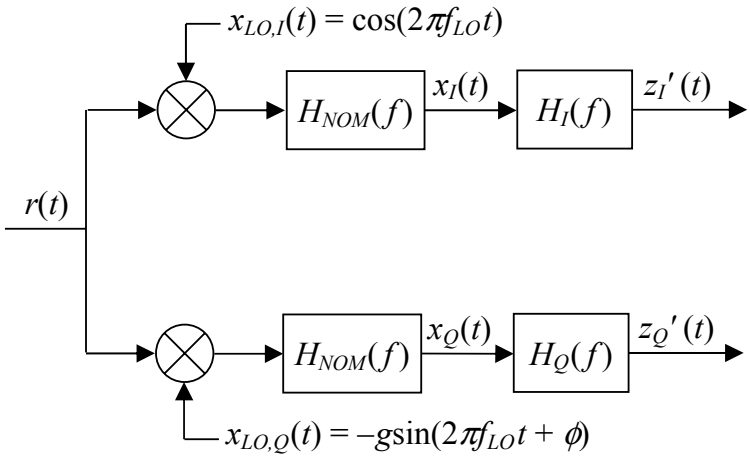

– **The effect of quadrature demodulator:** the local oscillator signal $x_{LO}(t)$ of an imbalanced quadrature demodulator is here modelled as

$$x_{LO}(t) = \cos(2\pi f_{LO}t) - jg\sin(2\pi f_{LO}t + \phi)$$
$$= K_1 e^{-j2\pi f_{LO}t} + K_2 e^{j2\pi f_{LO}t}$$

where g and ϕ represent the demodulator amplitude and phase imbalances, respectively.

– The mismatch coefficients K_1 and K_2 are given by

$$K_1 = [1 + ge^{-j\phi}]/2 \overset{ideally}{=} 1,$$
$$K_2 = [1 - ge^{j\phi}]/2 \overset{ideally}{=} 0.$$

– For more details, see the narrowband case in the beginning of the material (use $g \leftarrow -g$).

– **The effect of branch components:** the branch component mismatches can be easily modelled as imbalanced lowpass filters (LPF) as given by

$$H_{LPF,I}(f) = H_{NOM}(f)H_I(f)$$
$$H_{LPF,Q}(f) = H_{NOM}(f)H_Q(f)$$

– $H_{NOM}(f)$ is the nominal LPF response rejecting the high-frequency components.

– $H_I(f)$ and $H_Q(f)$ represent the actual mismatch effects due to branch filters, AGCs, A/Ds, etc.

→ with perfect matching (ideal case), $H_I(f) = H_Q(f)$

– Now, to explicitly characterize **the imbalance effects on the individual channel signals**, we write the multichannel received signal $r(t)$ as

$$r(t) = 2\,\mathrm{Re}[z(t)e^{j2\pi f_{LO}t}] = z(t)e^{j2\pi f_{LO}t} + z^*(t)e^{-j2\pi f_{LO}t}$$

– As a model, the received signal $r(t)$ is **down-converted** to baseband by mixing it with $x_{LO}(t)$.

– Assuming that $H_{NOM}(f) = 1$ for $|f| \le B/2$ and $H_{NOM}(f) = 0$ for $|f| > B/2$, the downconverted signal $x(t)$ can be easily written as

$$x(t) = K_1 z(t) + K_2 z^*(t)$$

– To analyze the effect of **branch mismatches**, the signal $x(t)$ can first be written as $x(t) = x_I(t) + jx_Q(t)$, where

$$x_I(t) = z_I(t)$$
$$x_Q(t) = g\cos(\phi)z_Q(t) - g\sin(\phi)z_I(t)$$

– Then, in terms of Fourier transforms, the signal $z'(t) = z_I'(t) + jz_Q'(t)$ after branch mismatches is given by

$$
\begin{aligned}
Z'(f) &= Z'_I(f) + jZ'_Q(f) \\
&= H_I(f)X_I(f) + jH_Q(f)X_Q(f) \\
&= H_I(f)Z_I(f) + jH_Q(f)[g\cos(\phi)Z_Q(f) - g\sin(\phi)Z_I(f)] \\
&= [H_I(f) - jH_Q(f)g\sin(\phi)]Z_I(f) + j[H_Q(f)g\cos(\phi)]Z_Q(f). \\
&= A_I(f)Z_I(f) + jA_Q(f)Z_Q(f)
\end{aligned}
$$

– After some manipulation, the above result can be written in a more convenient form as (see the general theorem in the wideband imbalance model section)

$$Z'(f) = G_1(f)Z(f) + G_2(f)Z^*(-f)$$

where

$$
\begin{aligned}
G_1(f) &= [A_I(f) + A_Q(f)]/2 \\
&= [H_I(f) + H_Q(f)ge^{-j\phi}]/2
\end{aligned}
$$

$$
\begin{aligned}
G_2(f) &= [A_I(f) - A_Q(f)]/2 \\
&= [H_I(f) - H_Q(f)ge^{j\phi}]/2
\end{aligned}
$$

– In the above model, the term relative to $Z^*(-f)$ is caused by the imbalances and represents **the image aliasing effect**.
  → with perfect matching, I/Q processing allows us to consider negative and positive frequencies separately
  → this separabililty of negative and positive frequencies (the ideal case) is lost due to mismatches

– Now, **the image attenuation of the analog front-end** can be defined as

$$L(f) = |G_1(f)|^2 \,/\, |G_2(f)|^2$$

– With practical analog electronics (as stated earlier), this attenuation is usually in the order of $20\ldots40$ dB.

– The important question is **whether this 20…40 dB attenuation is sufficient**
  → depends on the architecture
    → direct-conversion (zero-IF) receiver: sufficient, especially with low-order modulations
    → low-IF receiver: insufficient, even though the system specs help to some extent
    → general wideband receiver: clearly insufficient

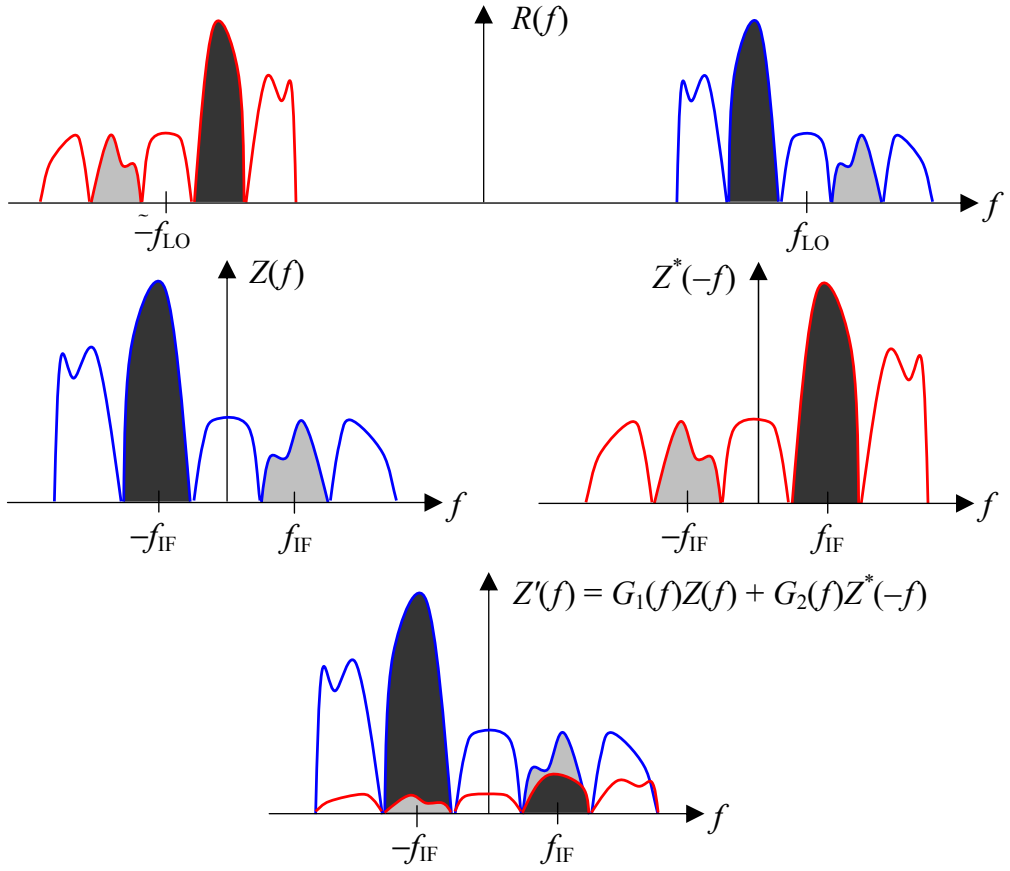

– **Possible solutions to enhance the image attenuation:**
  → analog RF image reject filtering (real or complex)
    → difficult to implement, complicates the analog front-end
    → limits the integrability
    → limits the flexibility
  → **advanced DSP at baseband** (referred to as imbalance compensation)
    → estimate the amplitude and phase mismatches and correct them
      → training signals needed usually
      → difficulties with frequency-selective mismatches
    → **novel statistical signal processing based methods to remove the image interference**
      → signal estimation vs. mismatch estimation
      → basic tools: adaptive interference cancellation or blind signal separation
      → blind, i.e., no training signals needed
      → can easily cope with frequency- and time-dependent imbalances
      → to be introduced next

4. ADVANCED DSP FOR I/Q IMBALANCE COMPENSATION

Baseband Signal Model for Digital Imbalance Compensation

– Here, in our formulation, **the task of imbalance compensation is to enhance the finite image attenuation $L(f)$ of the analog processing**.

– More precisely, **the target is to obtain an image-free observation of a specific channel** (referred to as the desired channel) **signal** located at non-zero intermediate frequency (IF) after the initial wideband downconversion

→ this signal estimation based approach is different from traditional imbalance compensation techniques

- traditional approach is to try to estimate the imbalance parameters and use them in some kind of a correction network
- here we directly estimate the final "quantity of interest"; the desired signal

– Some notations

→ desired channel (grey) baseband equivalent signal $s(t)$

→ image channel (dark) baseband equivalent signal $i(t)$

→ $P_X = E(|x(t)|^2)$ in general

– As in the ideal (perfect matching) case, the imbalanced multichannel signal $Z'(f)$ contains a

→ desired signal component around $+f_{IF}$

→ an image component around $-f_{IF}$

– Due to imbalances (see the previous figure), $Z'(f)$ has

→ also a destructive image signal component around $+f_{IF}$

→ also a desired signal component around $-f_{IF}$

– Motivated by this, we generate **two** baseband observations, $d(t)$ and $v(t)$

→ $d(t)$ is the baseband observation of the combined signal around $+f_{IF}$

→ $v(t)$ is the mirrored (complex-conjugated) baseband observation of the combined signal around $-f_{IF}$

→ this observation generation is illustrated in the following figure

→ the desired signal $s(t)$ is then estimated as

$$\hat{s}(t) = L\{d(t), d(t-1), d(t-2), ..., v(t), v(t-1), v(t-2), ...\}$$

→ what kind of processing $L\{.\}$ is used, is not defined yet

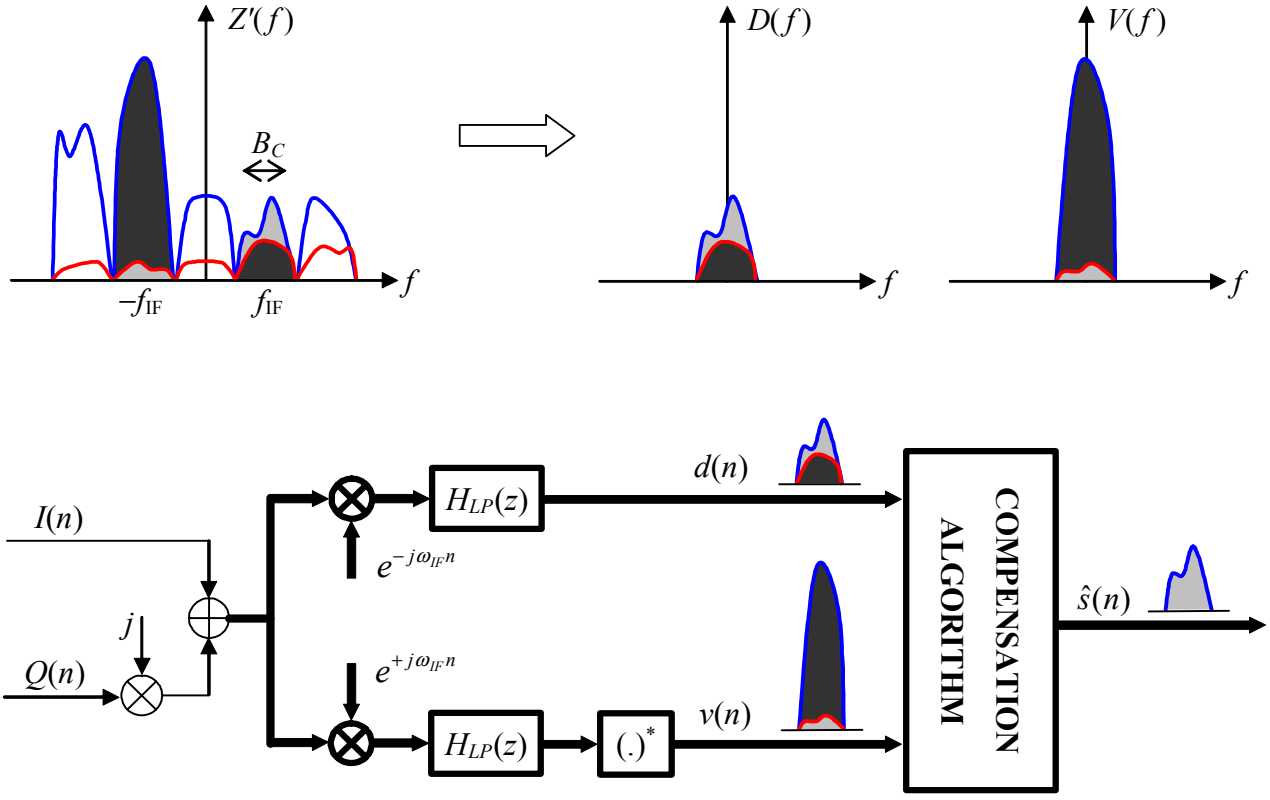

– After some manipulation, the frequency domain expression for these observations can be written using matrix formulation as

$$\mathbf{X}(f) = \mathbf{A}(f)\mathbf{S}(f)$$

where $\mathbf{X}(f) = [D(f)\ V(f)]^T$, $\mathbf{S}(f) = [S(f)\ I^*(-f)]^T$, and $s(t)$ and $i(t)$ denote the baseband equivalents of the desired and image signals, respectively.

– The matrix $\mathbf{A}(f)$ is given by

$$\mathbf{A}(f) = \begin{bmatrix} G_1(f+f_{IF}) & G_2(f+f_{IF}) \\ G_2^*(-f-f_{IF}) & G_1^*(-f-f_{IF}) \end{bmatrix} \mathbf{P}(f, B_C)$$

where B_C denotes the individual channel bandwidth and $\mathbf{P}(f,B_C) = diag[\Pi(f,B_C), \Pi(f,B_C)]$ with $\Pi(f,B_C) = 1$ for $|f| \le B_C/2$ and zero otherwise.

– If $H_I(f) = H_Q(f)$, the general model reduces to an instantaneous mixture model

$$\begin{bmatrix} d(t) \\ v(t) \end{bmatrix} = \begin{bmatrix} K_1\sqrt{P_S} & K_2\sqrt{P_I} \\ K_2^*\sqrt{P_S} & K_1^*\sqrt{P_I} \end{bmatrix} \begin{bmatrix} s_1(t) \\ s_2(t) \end{bmatrix}$$

where $s_1(t) = s(t)/\mathrm{sqrt}(P_S)$, $s_2(t) = i^*(t)/\mathrm{sqrt}(P_I)$, and $P_X = E(|x(t)|^2)$ in general.

– This is a valid model if the I/Q demodulator is the main source of imbalance.

– Notice that compensation is actually needed only if the image signal is more powerful than the desired signal, i.e.,

  → $\hat{s}(t) = d(t)$ is a good estimator if $P_S >> P_I$

– Even though the baseband model was here derived in continuous-time domain, the observations can in practice be generated digitally (after A/D)

  → excess imbalance effects are avoided

– Consequently, discrete-time notations $d(n)$, $v(n)$, $s(n)$, and $i(n)$ are used hereafter.

– In general, the observations $x_1(n) = d(n)$ and $x_2(n) = v(n)$ appear as convolutive mixtures of the effective source sequences $s_1(n) = s(n)$ and $s_2(n) = i^*(n)$

  → the instantaneous mixture model is a special case of this

Adaptive Interference Cancellation (IC) Based Compensation

– If the desired channel signal is originally more powerful than the image signal ($P_S >> P_I$), the image attenuation of analog processing is sufficient

  → the desired channel observation $d(n)$ can be used directly as an estimate of $s(n)$

– On the other hand, in the difficult case of a strong image signal ($P_I >> P_S$),

  → the attenuation of analog processing is insufficient

  → $v(n)$ is highly correlated with the interfering signal component (see the previous figure) but only weakly correlated with the desired signal component of $d(n)$

– Motivated by this, adaptive **interference canceller** can be used to estimate $s(n)$ as

$$\hat{s}_{IC}(n) = d(n) - \sum_{k=0}^{N_{IC}} w_k(n) v(n-k)$$

– The filter coefficients $w_k(n)$, $k = \{0, \ldots, N_{IC}\}$, can be adapted with any practical algorithm, such as the well-known least-mean-square (LMS) or recursive least-squares (RLS) algorithms.

Multichannel Blind Deconvolution (MBD) Based Compensation

– Assumption: Signals in different frequency channels are statistically independent.

– Observation: With practical imbalance values, the general mixture model is invertible (i.e., $\mathbf{A}(f)$ is non-singular).

→ **blind signal separation** (or multichannel blind deconvolution in general) algorithms can be used to estimate the source vector $\mathbf{s}(n) = [s(n)\ i^*(n)]^T$ as

$$\hat{\mathbf{s}}(n) = \sum_{k=0}^{N_{MBD}} \mathbf{W}_k(n)\mathbf{x}(n-k)$$

where $\mathbf{x}(n) = [d(n)\ v(n)]^T$.

→ the actual desired channel signal $s(n)$ is then estimated as

$$\hat{s}_{MBD}(n) = \mathbf{e}_i^T \hat{\mathbf{s}}(n),\ i = 1 \text{ or } 2,$$

where $\mathbf{e}_1 = [1\ 0]^T$ or $\mathbf{e}_2 = [0\ 1]^T$ is used, depending on the possible source permutation (i.e., MBD produces also an estimate of the image signal).

– In general, there exists a wide variety of different approaches to measure the independence of the separated output signals, and thus, to adapt the demixing matrices $\mathbf{W}_k(n)$, $k = \{0, \ldots, N_{MBD}\}$.

Comparisons

– In general, the IC based compensator is only utilizable if the image signal is more powerful than the desired channel signal.

– Consequently, some kind of power estimation of the different channel signals is needed to decide when to switch the IC structure on and off.

– This problem, usually referred to as signal leakage, can in theory be avoided using the MBD based compensator, though, no compensation is actually needed if the image signal is weak.

– On the other hand, the performance of the IC based solution is likely to be more insensitive to the effects of additive noise and symbol timing errors, and, especially, to different interferer types.

– Naturally, there is also the issue of computational complexity.

– **Both techniques**

→ are blind, i.e., no training signals needed !!

→ are able to handle frequency-selective mismatches

→ are also able to cope with time-variant mismatch effects due to inherent adaptive nature

Simulation Example

– Front-End Parameters:

→ The received signal consists of the desired and image channels of bandwidth 0.2π located originally around 0.7π and 0.3π, respectively.

→ The desired and image signals are QPSK- and 8PSK-modulated, respectively, with raised-cosine pulse-shapes (roll-off 0.35).

→ The relative power difference is -40 dB.

→ In translating the desired channel signal to an IF of 0.2π, imbalance values of $g = 1.02$ and $\phi = -2°$ are used for the quadrature demodulator.

→ After that, the branch mismatches are modelled as $H_I(z) = 0.01 + z^{-1} + 0.01z^{-2}$ and $H_Q(z) = 0.01 + z^{-1} + 0.2z^{-2}$.

→ Finally, the symbol rate baseband observations $d(n)$ and $v(n)$ are generated by proper frequency translations of $\pm 0.2\pi$, lowpass filtering, and decimation.

– IC Simulation:

→ The standard RLS algorithm with a forgetting factor of 0.999 is used to adapt the IC filter of length 5 ($N_{IC} = 4$).

→ The total number of samples is $2{,}000$ to guarantee steady-state operation.

– MBD Simulation:

→ The natural gradient based algorithm of Amari et al. is used with a step-size of 0.001 to adapt the demixing filters of length 5 ($N_{MBD} = 4$).

→ The total number of samples is $12{,}000$ to quarantee steady-state operation.

→ To stabilize the adaptation, the source separator input signals $x_1(n) = d(n)$ and $x_2(n) = v(n)$ are normalized as (ad-hoc)

$$x_1(n) \leftarrow x_1(n)/\mathrm{sqrt}(P_1),$$

$$x_2(n) \leftarrow x_2(n)/\mathrm{sqrt}(P_2),$$

where the power estimates $P_1(n)$ and $P_2(n)$ are obtained recursively as

$$P_i(n) = 0.995P_i(n-1) + 0.005|x_i(n)|^2,\ i = 1 \text{ and } 2.$$

– Comments:

→ Front-end imbalance properties used in the simulations are illustrated in Figure 1 and Figure 2.

→ Single realizations of the absolute value of the "center taps" $w_2(n)$ and $W_{2,ij}(n) = [\mathbf{W}_2(n)]_{ij}$ are presented in Figure 3 and Figure 4 to illustrate the convergence properties.

→ Clearly, the IC algorithm converges much faster than the MBD algorithm.

→ However, as verified by Figure 5, there is no difference in the steady-state operation between the two methods (only the desired signal estimate is shown for the MBD method, it also produces an estimate of the original image signal).

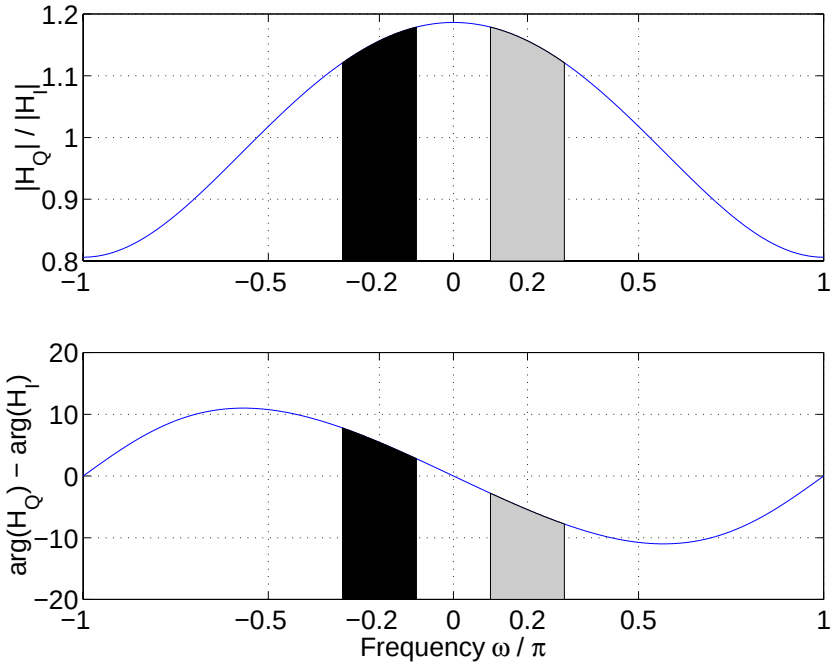

Figure 1. Relative amplitude and phase mismatches of the branch components. Positive (*grey*) and negative (*dark*) IF bands are illustrated in different colours.

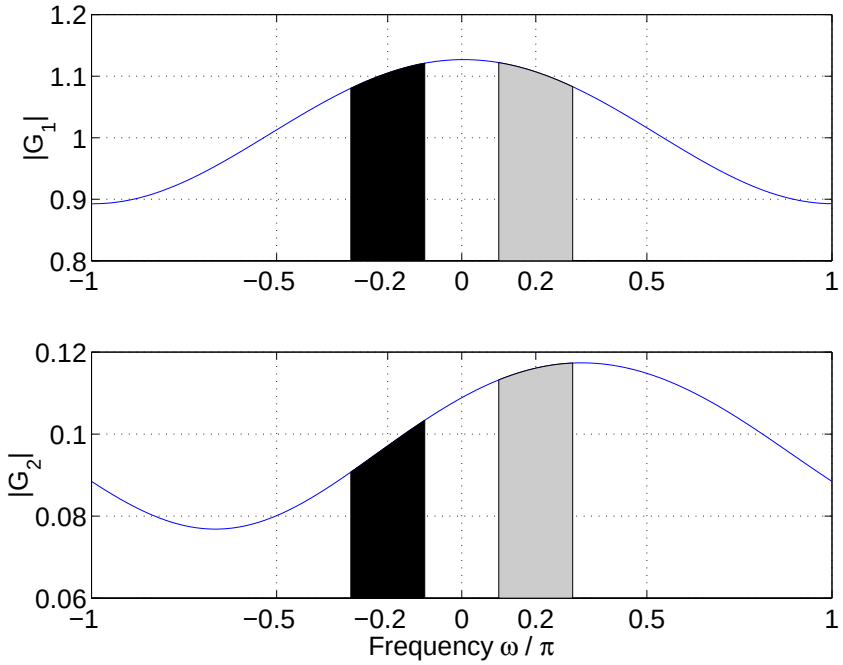

Figure 2. General imbalance coefficients G_1 and G_2. Positive (*grey*) and negative (*dark*) IF bands are illustrated in different colours.

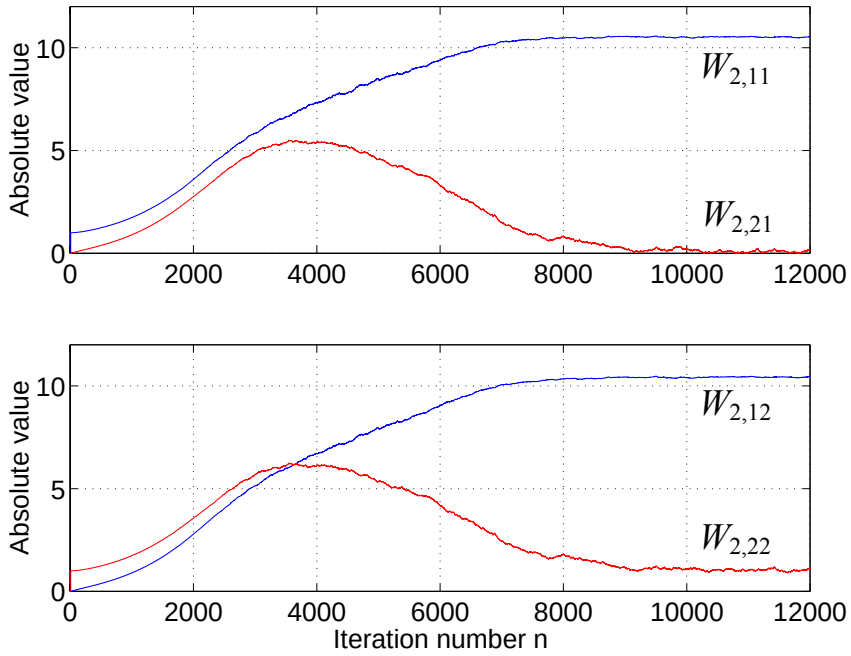

Figure 3. Center tap values $W_{2,ij}(n) = [\mathbf{W}_2(n)]_{ij}$ of the demixing filters using the natural gradient algorithm (step-size 0.001).

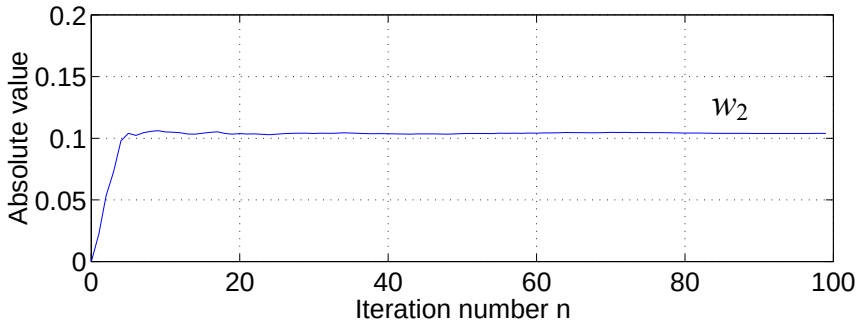

Figure 4. Center tap value $w_2(n)$ of the RLS (forgetting factor 0.999) based interference canceller.

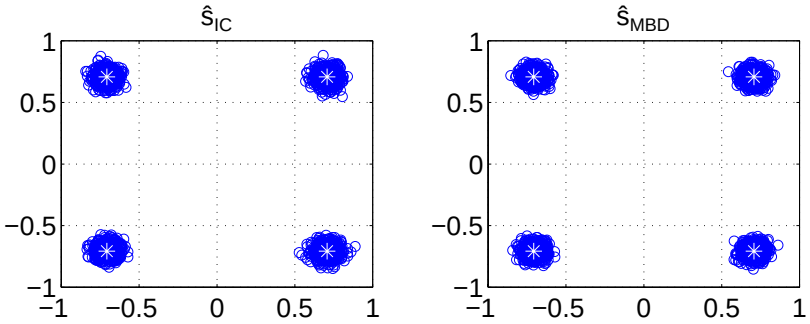

Figure 5. Compensated output samples after convergence of both the IC (*left*) and MBD (*right*) based compensators. Also shown are the ideal QPSK symbol locations (*white asterisks*).

5. Second-Order Sampling and Enhancements

– **Starting point:** Complex (I/Q) sampling of bandpass signals.

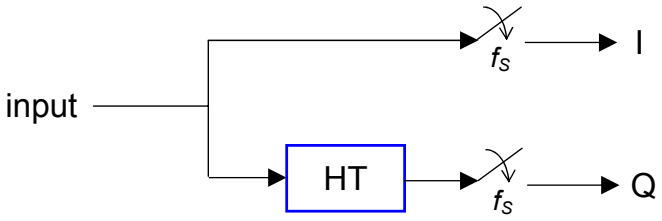

– **Idea:** Approximate the needed 90 degree phase shift (Hilbert transformer) using a simple time delay of one quarter of the carrier cycle.

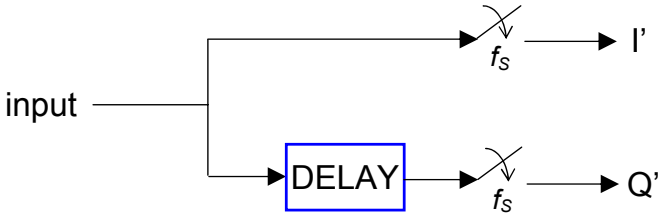

– The time delay of $\Delta T = 1/(4f_C)$ corresponds to a **frequency-dependent phase shift** of

$$-2\pi f \Delta T = -\frac{\pi}{2}\frac{f}{f_C}$$

→ thus the ideal Hilbert filtering is achieved only at the carrier-frequency $\pm f_C$

→ as a result, the supression of the negative frequency content (image components) is generally imperfect

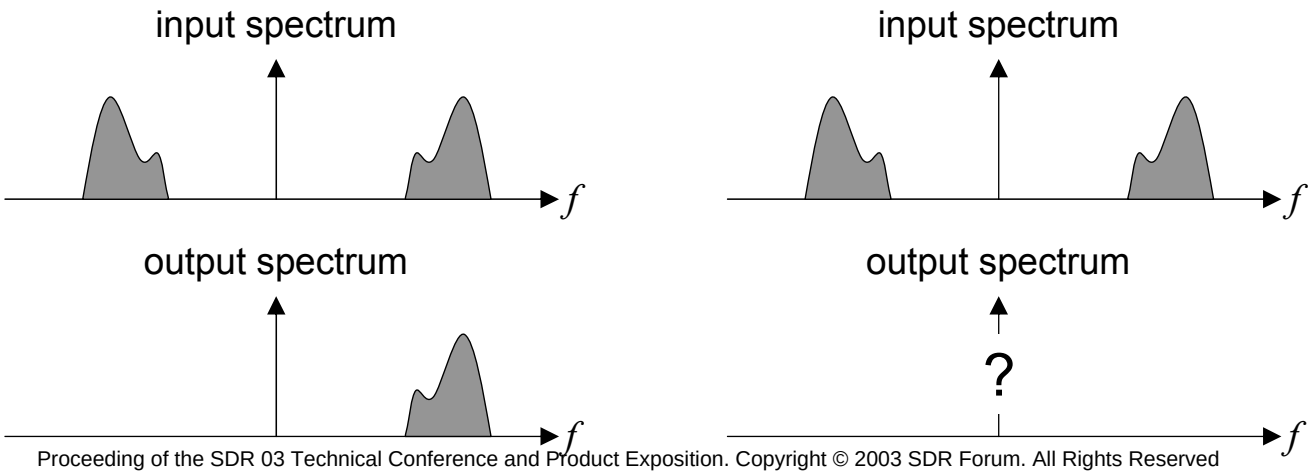

Filtering Effect of the Delay Processing

– We write the input bandpass signal $r(t)$ in terms of its baseband equivalent signal $z(t) = z_I(t) + jz_Q(t)$ as (scaling by 2 is irrelevant and could be ignored)

$$r(t) = 2\,\mathrm{Re}[z(t)e^{j2\pi f_C t}] = z(t)e^{j2\pi f_C t} + z^*(t)e^{-j2\pi f_C t}$$
$$= 2z_I(t)\cos(2\pi f_C t) - 2z_Q(t)\sin(2\pi f_C t)$$

– Then the complex signal, say $x(t)$, entering the sampler(s) is generally of the form $x(t) = r(t) + jr(t - \Delta T)$ where $\Delta T = 1/(4f_C)$.

– The spectrum of this signal can be written as

$$X(f) = [1 + jH_D(f)]R(f)$$

where

$$H_D(f) = e^{-j2\pi f \Delta T}.$$

– This effect is illustrated in frequency domain in the following figure.

WITH HILBERT TRANSFORMER

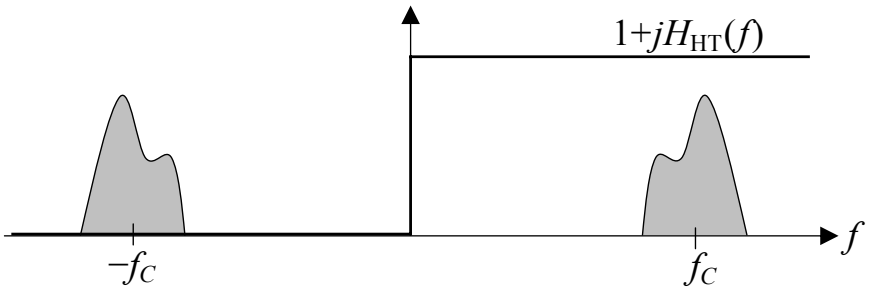

WITH DELAY

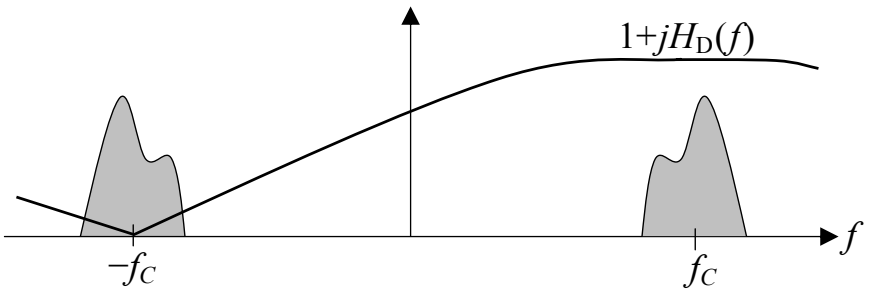

– Now suppose you use a subharmonic sampling frequency $f_S = f_C / r$, where the integer $r \geq 1$ denotes the subsampling ratio.
  → the signal is aliased directly to baseband
  → **in case of delay processing, the component from negative frequencies falls directly on top of the desired component**
    - kind of self-interference
    - actually depends on the structure of the signal
      - in case of a single frequency channel (as shown below), this interference is not really problematic, especially with low-order modulations
      - but how about in the wideband/multichannel case ?

WITH HILBERT TRANSFORMER

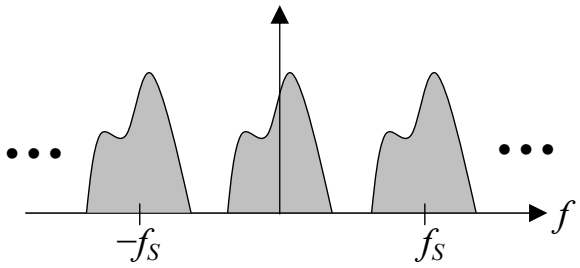

WITH DELAY

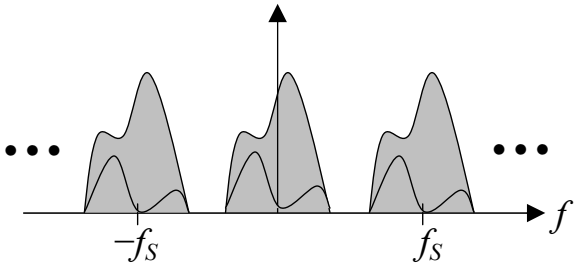

– When applied to multichannel signals, the **image band signal** ban be much more powerful than the desired channel
  → obvious problem
  → quantitative measures given shortly

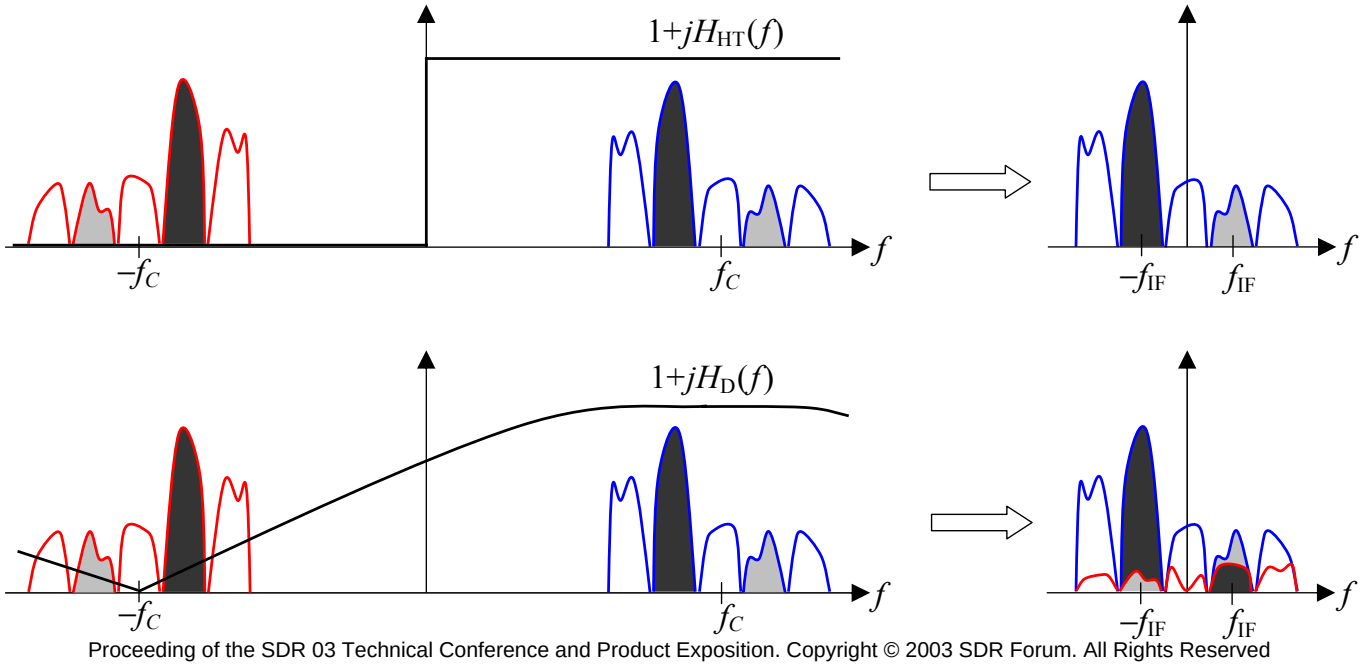

Image Attenuation Analysis

– After some manipulations, the sampled complex signal (with $f_S = f_C / r$, r integer) can be written as

$$\begin{aligned} x(nT_S) &= r(nT_S) + jr(nT_S - \Delta T) \\ &= \ldots \\ &= 2z_I(nT_S) + j2z_Q(nT_S - \Delta T) \\ &= I'(n) + jQ'(n) \end{aligned}$$

– Thus it is interesting to note that the **front-end delay maps directly into a corresponding delay of the baseband observation**.

– For analysis purposes, we can formally think that the discrete-time signal is obtained by sampling the corresponding continuous time baseband signal

$$z'(t) = 2z_I(t) + j2z_Q(t - \Delta T)$$

– This can be written in a more informative form as

$$z'(t) = z(t) + z(t - \Delta T) + z^*(t) - z^*(t - \Delta T)$$

→ the part including $z(t)$ and $z(t-\Delta T)$ corresponds to the signal component originating from **positive** frequencies

→ the part including $z^*(t)$ and $z^*(t-\Delta T)$ corresponds to the signal component originating from **negative** frequencies

– To get the exact image attenuation, we write the Fourier Transform of $z'(t)$ as

$$Z'(f) = (1 + e^{-j2\pi f \Delta T})Z(f) + (1 - e^{-j2\pi f \Delta T})Z^*(-f)$$

– Then, the image attenuation $L_2(f)$ provided by the second-order sampling is given by

$$L_2(f) = \frac{\left|1 + e^{-j2\pi f \Delta T}\right|^2}{\left|1 - e^{-j2\pi f \Delta T}\right|^2} = \ldots = \left| \frac{1 + \cos(2\pi f \Delta T)}{\sin(2\pi f \Delta T)} \right|^2$$

– To illustrate, if the center frequency $f_C = 100$ MHz and the bandwidth $B = 25$ MHz, the image attenuation $L_2(f)$ at the band edge is only around 20 dB

→ in case of multichannel downconversion, the power difference of the individual channel signals can be even $50 \ldots 100$ dB

→ then, it is clear that the image attenuation $L_2(f)$ and thus, the basic second-order sampling scheme, are not sufficient as such for multichannel receivers!!

Second-Order Sampling and Enhanced Image Rejection

- In narrowband single channel receivers, the image signal is inherently a "self-image" and the attenuation of the basic second-order sampling scheme as such can be adequate.
- In multichannel receivers, as discussed before, the image band signal can be up to 50-100 dB stronger than the desired channel signal, and the image attenuation of the basic second-order scheme alone is clearly insufficient.
- **Two alternative methods to enhance this image attenuation are presented next.**
- For simplicity, the following compensation methods are analyzed in continuous-time domain.

Interference Cancellation

- **The basic idea:** To enhance the obtainable image attenuation, and thus, to reproduce an accurate baseband observation of the multichannel signal $z(t)$, the interference canceller –type of compensation structure is proposed.

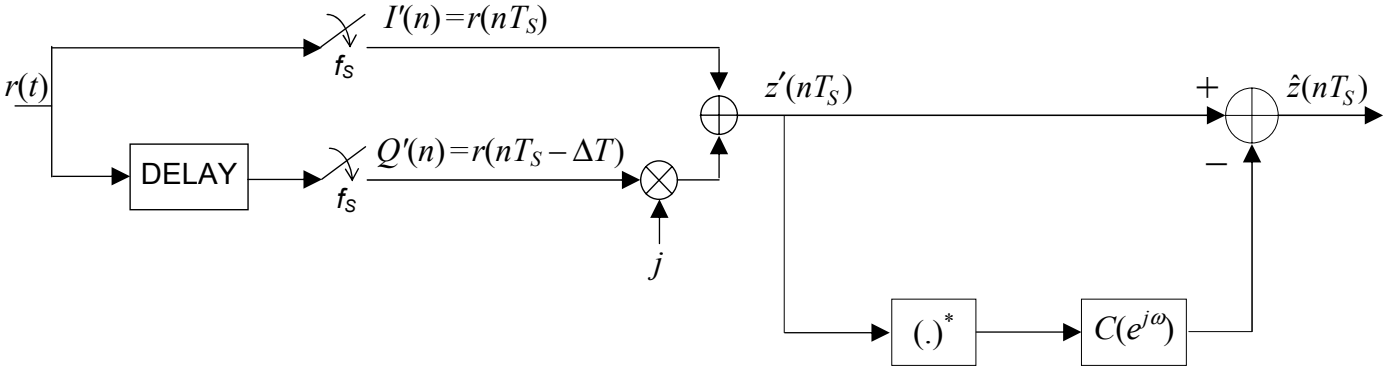

– As illustrated, the idea is to use a fixed compensation filter $C(f)$ together with the complex conjugate of $z'(t)$ as a reference signal to estimate and subtract the image signal interference.

– Based on the previous signal model for $Z'(f)$ and on the proposed compensation strategy, the frequency response of $\hat{z}(t)$ can be written as

$$\begin{aligned}\hat{Z}(f) &= Z'(f) - C(f)Z'^{*}(-f) \\ &= G_{1,IC}(f)Z(f) + G_{2,IC}(f)Z^{*}(-f)\end{aligned}$$

where

$$G_{1,IC}(f) = 1 + e^{-j2\pi f\Delta T} - C(f)(1 - e^{-j2\pi f\Delta T})$$

$$G_{2,IC}(f) = 1 - e^{-j2\pi f\Delta T} - C(f)(1 + e^{-j2\pi f\Delta T})$$

– As a result, the image signal components of $\hat{z}(t)$ are attenuated with respect to the desired signal components by

$$L_{IC}(f) = \frac{|G_{1,IC}(f)|^2}{|G_{2,IC}(f)|^2}$$

– Then, to completely cancel the image signal components, the compensator frequency response $C(f)$ should be selected in such a way that $G_{2,IC}(f) = 0$.

– This solution, referred to as the "zero forcing" –solution $C_{ZF}(f)$, is given by

$$C_{ZF}(f) = \frac{1 - e^{-j2\pi f\Delta T}}{1 + e^{-j2\pi f\Delta T}}.$$

– After some manipulation, this can be written as

$$C_{ZF}(f) = \frac{j\sin(2\pi f\Delta T)}{1 + \cos(2\pi f\Delta T)}.$$

– The above frequency response can be well approximated using a real-valued impulse response with odd symmetry.

– Therefore, no "cross-filtering" between the I and Q components of the input signal $z'(t)$ is needed.

– Using this optimum compensator, the gain $G_{1,ZF}(f)$ of the desired signal components can be easily shown to be of the form

$$G_{1,ZF}(f) = 1 + e^{-j2\pi f\Delta T} - C_{ZF}(f)(1 - e^{-j2\pi f\Delta T}) = \frac{4e^{-j2\pi f\Delta T}}{1 + e^{-j2\pi f\Delta T}}.$$

- With reasonable bandwidth-to-center frequency ratios (B / f_C), this describes practically a constant gain, linear phase frequency response.
- As a consequence, the effect of image components $Z^*(-f)$ can indeed be successfully compensated without causing any notable distortion to the desired components $Z(f)$.
- Thus, an accurate reproduction of $z(t)$ is obtained, i.e., $\hat{z}(t) \approx z(t)$ (up to a delay and multiplication by a constant).
- In the actual digital implementation, $C_{ZF}(f)$ gives the desired response which should be approximated using a finite order discrete-time FIR/IIR filter.
- This can be done, e.g., using a type III FIR filter (odd symmetry).
- A **design example** is given below:
  → $f_C = 100$ MHz, $B = 25$ MHz, $f_S = 50$ MHz
  → type III FIR filter, length 9, LS and minimax approximations of the given optimum response

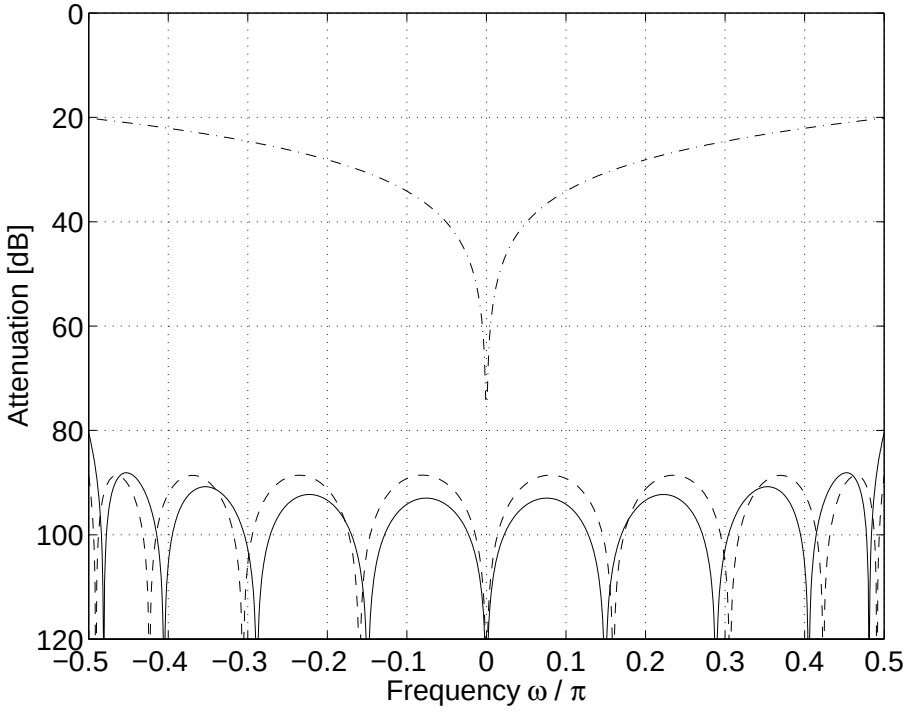

- *dash-dotted*: basic second-order sampling (L_2)
- *solid*: enhanced scheme with LS –optimized IC compensation filter (L_{IC})
- *dashed*: enhanced scheme with minimax –optimized IC compensation filter (L_{IC})

Fractional-Delay Filtering

- Motivated by the original signal model, the image attenuation of the basic second-order sampling scheme can also be enhanced by properly delaying the I branch signal $r(nT_S)$ relative to the Q branch signal $r(nT_S - \Delta T)$.
- Using a sampling frequency $f_S = f_C / r$, the needed delay $\Delta T = T_S/(4r)$ is only a fraction of the sampling interval T_S.
- Therefore, a digital fractional delay filter $D(z)$ is a natural choice for the delay implementation.
- The basic block-diagram of the modified second-order sampling based quadrature demodulator utilizing this idea is presented below.

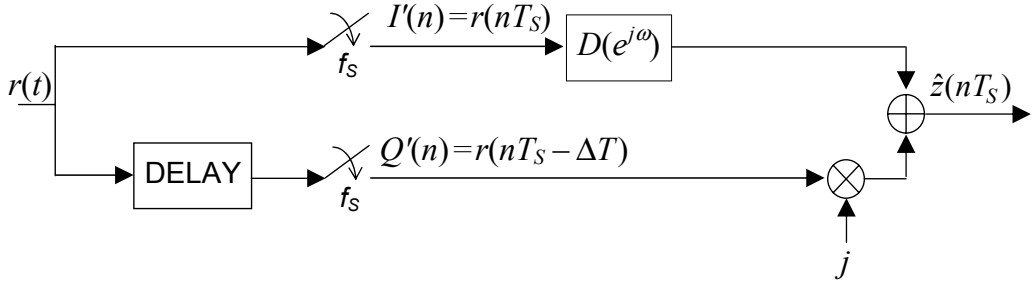

- To analyze the **image attenuation** of the complete structure, we proceed as follows (in continuous-time domain for simplicity).
- First, let $D(f)$ denote the frequency response of the fractional delay compensation filter.
- Then, the Fourier transform of the compensated signal $\hat{z}(t)$ is given by

$$\hat{Z}(f) = 2Z_I(f)D(f) + j2Z_Q(f)e^{-j2\pi f\Delta T}$$

- After some manipulations, this can be written in a more convenient form as

$$\hat{Z}(f) = G_{1,FD}(f)Z(f) + G_{2,FD}(f)Z^*(-f)$$

where

$$G_{1,FD}(f) = D(f) + e^{-j2\pi f\Delta T}$$

$$G_{2,FD}(f) = D(f) - e^{-j2\pi f\Delta T}$$

- As a result, the enhanced image attenuation $L_{FD}(f)$ of fractional delay processing is given by

$$L_{FD}(f) = \frac{\left|G_{1,FD}(f)\right|^2}{\left|G_{2,FD}(f)\right|^2} = \frac{\left|D(f) + e^{-j2\pi f\Delta T}\right|^2}{\left|D(f) - e^{-j2\pi f\Delta T}\right|^2}$$

– Naturally, the ideal frequency response of the needed fractional delay filter is, indeed, $e^{-j2\pi f\Delta T}$ for which $L_{FD} \to \infty$.

– Based on the previous analysis, this would result in a perfect (up to a delay and multiplication by a constant) reconstruction of the desired baseband equivalent signal as $\hat{z}(t) = 2z(t - \Delta T)$.

– Considering the actual digital implementation, let $\mu = \Delta T / T_S = 1/(4r)$ denote the normalized fractional delay.

– Then, the frequency response of the ideal digital FD filter is given by

$$D_{OPT}(e^{j\omega}, \mu) = e^{-j\omega\mu} \quad \text{for } |\omega| \le \pi B / f_S,$$

where $\omega = 2\pi f / f_S$.

– Again, the task is to approximate this ideal response using a finite order FIR/IIR filter.

– Previous **design example**:

→ $f_C = 100$ MHz, $B = 25$ MHz, $f_S = 50$ MHz ($\to \mu = 1/8$)

→ FIR filter, length 8, LS and minimax approximations of the given optimum response

→ results are illustrated in the following figure

– **General conclusion:** Based on the presented design examples, image attenuations in the order of 80 … 100 dB can be easily achieved (at least theoretically) using either of the presented techniques (IC/FD).

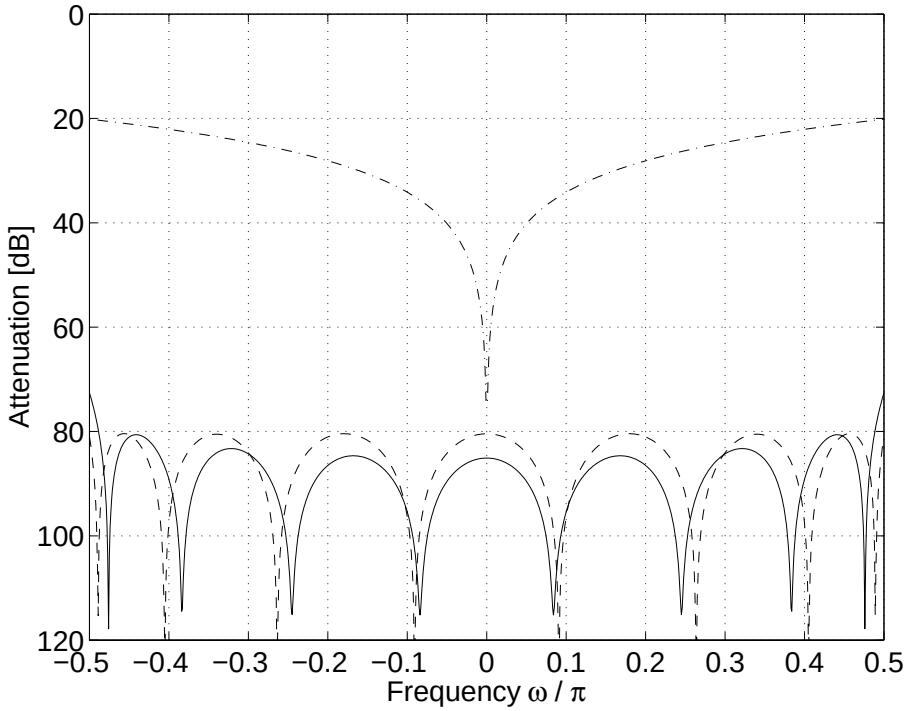

- *dash-dotted*: basic second-order sampling (L_2)
- *solid*: enhanced scheme with LS –optimized FD compensation filter (L_{FD})
- *dashed*: enhanced scheme with minimax –optimized FD compensation filter (L_{FD})

6. I/Q Signal Processing in Frequency Synthesizers

- The design of frequency synthesizers is challenging for wireless applications:
  → spectral purity, high frequency range, fast tuning, power consumption, etc.
- Here the idea of **combining digital and analog synthesis techniques** for achieving these goals is discussed and analyzed
  → the proposed architecture uses I/Q modulation to translate a digitally synthesized tuneable low frequency tone to the final frequency range
- **Practical problems:** unavoidable mismatches between the amplitudes and phases of the I and Q branches result in imperfect sideband rejection degrading the spectral purity of the synthesized signal.
- A **compensation structure** based on digital pre-distortion of the low frequency tone is presented to enhance the signal quality
  → practical algorithms for updating the compensator parameters are proposed based on minimizing the envelope variation of the synthesizer output signal
  → simulation results are also presented to illustrate the efficiency of the proposed synthesizer concept

Synthesizer Architecture

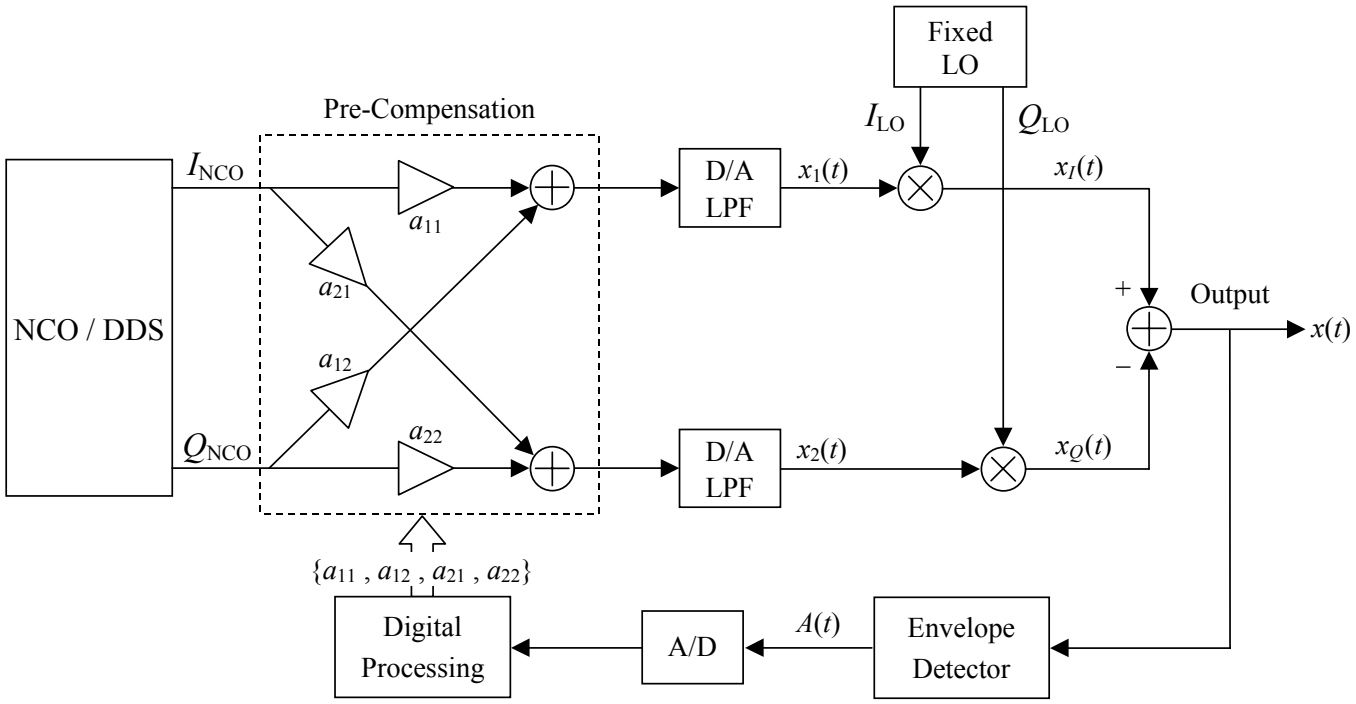

Figure. Synthesizer architecture where digital pre-compensation is used to compensate for the non-idealities of the analog part.

– **Signal Analysis:**

→ NCO signals: $I_{NCO}(t)=\cos(\omega_{NCO}t)$ and $Q_{NCO}(t)=\sin(\omega_{NCO}t)$

→ I/Q mixer: $I_{LO}(t)=\cos(\omega_{LO}t)$ and $Q_{LO}(t)=g\sin(\omega_{LO}t+\phi)$ where g and ϕ denote the gain and phase imbalances of the mixing stage

→ furthermore, let θ_1 and θ_2 denote the relative phase shifts due to the D/A converters and branch filters.

– Now, the synthesizer output signal $x(t)$ can be easily shown to be of the form $x(t)=\mathrm{Re}[x_{LP}(t)\exp(j\omega_{LO}t)]$ where the lowpass equivalent $x_{LP}(t)$ is given by

$$x_{LP}(t)=\alpha e^{j\omega_{NCO}t}+\beta e^{-j\omega_{NCO}t}$$

– Thus, **the synthesizer output consists of *two* spectral components:**

→ the desired tone at $\omega_{LO}+\omega_{NCO}$ and

→ the image tone at $\omega_{LO}-\omega_{NCO}$

whose relative strengts $|\alpha|^2$ and $|\beta|^2$ depend on g, ϕ, and $\theta=\theta_2-\theta_1$, as well as on the compensation parameters a_{ij}.

– With practical analog electronics, the image tone attenuation defined here as

$$L=|\alpha|^2/|\beta|^2$$

is only 20-40 dB if no compensation is used (i.e., $a_{11}=a_{22}=1$ and $a_{12}=a_{21}=0$)

→ in wireless systems, these levels of synthesizer spurious tones can result in severe interchannel interference (ICI)

→ in general, image tone attenuations in the order of 50-80 dB are needed in wireless applications

– **The image tone at the synthesizer output can, however, be canceled with proper pre-compensation parameters a_{ij}.**

– In fact, setting $\beta=0$ and $\alpha=\exp(j\theta_1)$ will force the output to be a pure sinusoidal (with relative phase θ_1).

– These optimum parameters a_{ij} can be easily shown to be of the form

$$a_{11}=1,\ a_{12}=\tan(\phi),\ a_{21}=-\frac{\sin(\theta)}{g\cos(\phi)},\ a_{22}=\frac{\cos(\theta)}{g\cos(\phi)}$$

– If the only motivation is really just to cancel the image tone (i.e., to set $\beta = 0$), a **more simple solution is also available**.

– Using the notation $\psi = \phi - \theta$, the solution can be formulated as

$$a_{11} = 1,\ a_{12} = \tan(\psi),\ a_{21} = 0,\ a_{22} = \frac{1}{g\cos(\psi)}$$

for which also $\alpha \approx \exp(j\theta_1)$ with practical imbalance values.

– **Thus, only two actual compensation parameters a_{12} and a_{22} need to be implemented.**

– Notice that only the **phase error difference** $\psi = \phi - \theta$ and the gain mismatch g are actually contributing to the image tone, and therefore, on the ideal compensation parameters.

Practical Compensator Update

– In practice, the imbalances g, ϕ, and θ needed to calculate the previous compensators are unknown and need to be measured or estimated somehow.

– To emphasize implementation simplicity, **the approach taken here is to carry out the estimation using only the envelope of the synthesizer output:**

$$A(t) = |x_{\mathrm{LP}}(t)| = |\alpha e^{j\omega_{\mathrm{NCO}}t} + \beta e^{-j\omega_{\mathrm{NCO}}t}| = \sqrt{|\alpha|^2 + |\beta|^2 + 2\,\mathrm{Re}[\alpha\beta^* e^{j2\omega_{\mathrm{NCO}}t}]}$$

→ the envelope is flat only if the image tone is completely attenuated ($\beta = 0$)

– **Thus, instead of estimating g and ψ, a more simple approach is to directly adapt a_{12} and a_{22} to minimize the envelope variation.**

– One possibility is to consider the envelope peak-to-peak (PP) value

$$d_A = \max\{A(t)\} - \min\{A(t)\}$$

– Given that $|\alpha| > |\beta|$, which is always the case with practical imbalance values, the above peak-to-peak value can also be expressed as

$$d_A = 2|\beta| = \sqrt{1 + g^2 a_{22}^2 + a_{12}^2 - 2ga_{22}(\cos(\psi) + a_{12}\sin(\psi))}\,.$$

– Though not strictly parabolic, the d_A -surface having a unique minimum lends itself well to iterative minimization.

– The true gradient of d_A (derivative with respect to a_{12} and a_{22}) depends, however, on g and ψ which are unknown.

– **A practical approach is then to adapt only one parameter (either a_{12} or a_{22}) at a time.**

– The direction (sign) of the needed one dimensional gradient at each iteration can be determined based on observing the behaviour of d_A between two previous adaptations of the corresponding parameter.

– Assuming that a_{12} and a_{22} are updated at odd and even adaptation instants, respectively, this leads to the following update rule

$$\hat{a}_{12}(n) = \hat{a}_{12}(n-2) + K_{12}(n)\lambda_1 \frac{d_A(n)}{\lambda_2 + d_A(n)}$$

$$\hat{a}_{22}(n) = \hat{a}_{22}(n-1)$$

for n odd with $K_{12} \in \{+1, -1\}$ and

$$\hat{a}_{12}(n) = \hat{a}_{12}(n-1)$$

$$\hat{a}_{22}(n) = \hat{a}_{22}(n-2) + K_{22}(n)\lambda_1 \frac{d_A(n)}{\lambda_2 + d_A(n)}$$

for n even with $K_{22} \in \{+1, -1\}$.

– In the above adaptation scheme, $K_{12}(n) = K_{12}(n-2)$ if $d_A(n-1) \leq d_A(n-2)$ and $K_{12}(n) = -K_{12}(n-2)$ if $d_A(n-1) > d_A(n-2)$ with similar reasoning for K_{22}.

– Step-size parameters $\lambda_1 > 0$ and $\lambda_2 \geq 0$ are used here to control the adaptation speed and steady-state accuracy. Notice that the magnitude of the update term is always between zero and λ_1, depending on the value of d_A.

Example Simulations

- To demonstrate the proposed synthesizer concept with digital pre-compensation, some computer simulations are carried out.
- In the simulations, imbalance values of $g=1.05$, $\phi=6°$, and $\theta=1°$ ($\psi=\phi-\theta=5°$) are used, corresponding to an image tone attenuation of approximately 26 dB.
- Pre-compensation parameters are initialized as $a_{12}=0$ and $a_{22}=1$ and are then iteratively updated one-by-one to minimize the peak envelope variation using the approach described above.
- In general, updating is carried out once per envelope cycle and step-size values of $\lambda_1=0.01$ and $\lambda_2=0.02$ are used.
- With these example values, the d_A -surface is illustrated in Figure 1 as a function of a_{12} and a_{22}.
- Also shown in the a_{12},a_{22} -plane is the behaviour of the pre-distortion parameters during one simulation realization.

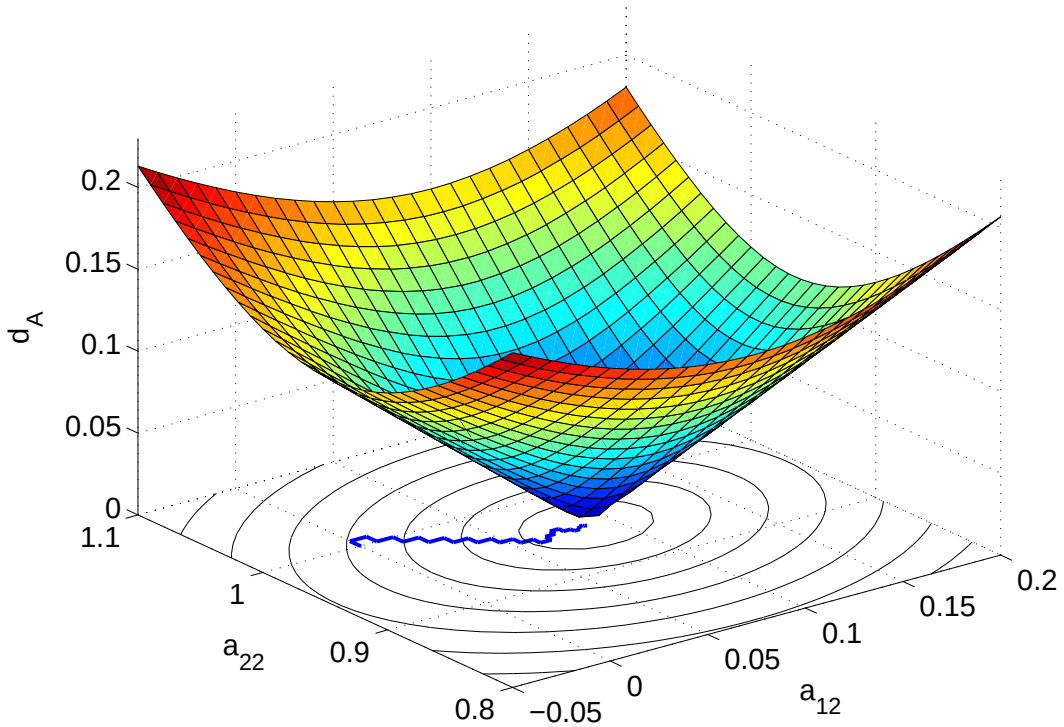

Figure 1: Peak envelope variation d_A as a function of the compensation parameters a_{12} and a_{22} for $g=1.05$ and $\psi=5°$. Also shown in the a_{12},a_{22} -plane is one realization of the compensation parameters during the adaptation.

– The corresponding output envelope is depicted in Figure 2 verifying successful synthesizer operation.

– With these imbalance and step-size values, the steady-state operation is reached in 50 iterations or so and the steady-state image attenuation is in the order of 100-150 dB.

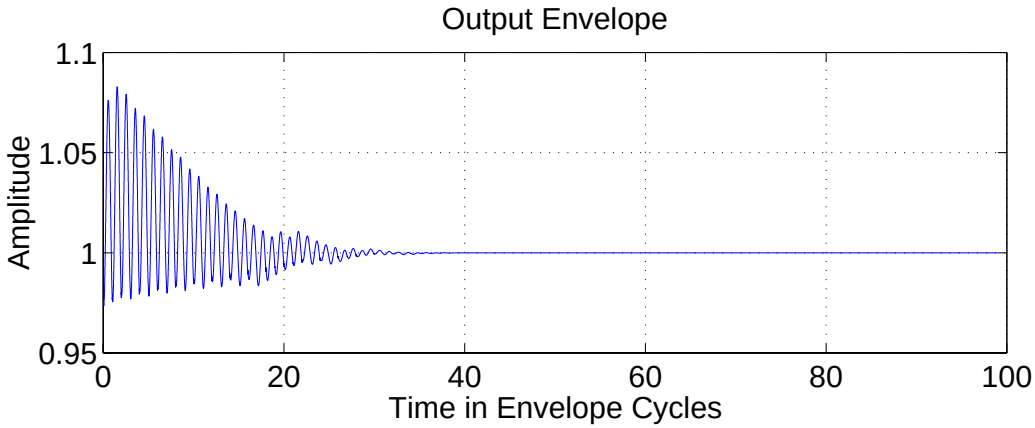

Figure 2: Envelope of the synthesizer output signal during the adaptation ($g = 1.05$ and $\psi = 5°$).

– To illustrate the ability to perform the compensation also in time-varying environments, an abrupt change in the imbalances is tested.

– The gain mismatch coefficient g is changed from 1.05 to 0.98 and the I/Q mixer phase imbalance ϕ from $6°$ to $4°$.

– The resulting output envelope is presented in Figure 3 evidencing fast and accurate synthesizer operation also in case of time-varying imbalances.

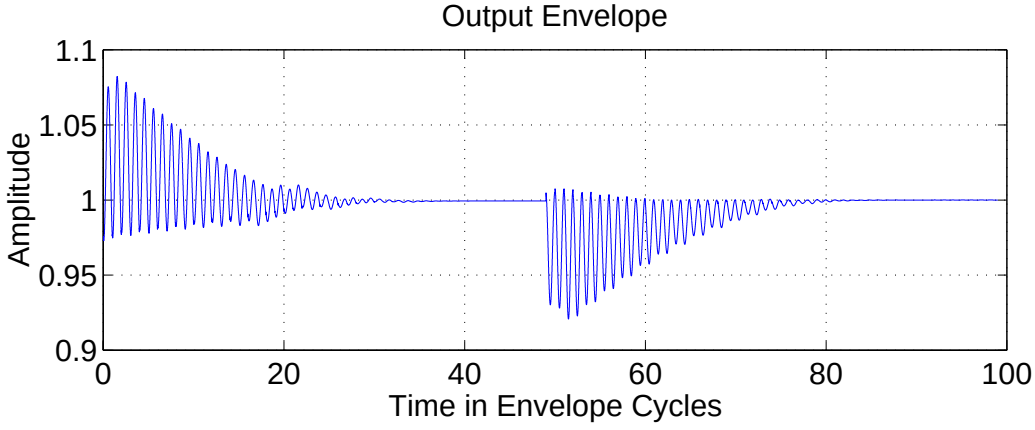

Figure 3: Envelope of the synthesizer output signal during the adaptation when the initial imbalances $g = 1.05$ and $\psi = 5°$ are changed to $g = 0.98$ and $\psi = 3°$, respectively.

Some Practical Matters

- The output envelope is periodic with fundamental frequency $2\omega_{\mathrm{NCO}}$
  - → if d_A is determined and compensation parameters updated once per envelope cycle (or once per several cycles), the frequency range of the digital synthesis part should be selected in such a manner that the envelope variation rate does not limit the whole synthesizer's settling time
  - → on the other hand, higher frequencies in the digital part always imply higher sampling rates and higher power consumption
  - → proper compromise between these two issues is needed
- Data and coefficient wordlengths:
  - → according to preliminary results, image tone attenuations in the order of 80 dB are achievable with 16 bits, more detailed analysis still needed
  - → one important issue in this context is also the available accuracy of the envelope variation measurements
- Local oscillator leakage: creates an additional spectral component at ω_{LO}, can be compensated by adding proper constants to the low frequency (NCO) signals.

Conclusions

- In this section, frequency synthesizer design for wireless applications was considered.
- To achieve fast switching capabilities with high operating frequencies and reasonable power consumption, the approach was to use I/Q modulation of digitally tunable low frequency tone.
- The practical imbalance problem with analog I/Q signal processing was then considered and analyzed.
- Based on this analysis, a digital pre-compensation structure was presented together with some simple yet efficient approaches to determine the compensator coefficients.
- The proper operation of the whole synthesizer was demonstrated using computer simulations both in time-invariant and time-varying situations.
- Future work should be directed to more detailed evaluation of the finite wordlength effects (hardware prototyping, etc.).

GENERAL SUMMARY

- Efficient processing of complex (I/Q) signals is the key in developing and building sophisticated communication systems.
- Frequency translations and advanced sampling techniques as well as efficient multirate DSP are good examples where complex signal concepts are especially useful
  - → Hilbert transform and the notion of analytic signals
  - → polyphase filtering
  - → second-order sampling and its enhancements
- One important practical aspect is the mismatch problem associated with analog I/Q signals
  - → image attenuation analysis
  - → digital compensation techniques
- Frequency synthesizers represent another interesting application where I/Q signal processing can be utilized.

SOME REFERENCES

[1] A. A. Abidi, "Direct conversion radio transceivers for digital communications," *IEEE J. Solid-State Circuits*, vol. 30, pp. 1399-1410, Dec. 1995.

[2] A. A. Abidi, "CMOS wireless transceiver: The new wave," *IEEE Commun. Mag.*, vol. 37, pp. 119-124, Aug. 1999.

[3] A. A. Abidi, "Low-power radio-frequency ICs for portable communications," in L. E. Larson, Ed., *RF and Microwave Circuit Design for Wireless Communications*. Norwood, MA: Artech House, 1996, pp. 43-98.

[4] S. Amari, S. C. Douglas, A. Cichocki, and H. H. Yang, "Multi-channel blind deconvolution and equalization using the natural gradient," *in Proc. IEEE Workshop Signal Processing Adv. Wireless Commun.*, Paris, France, Apr. 1997, pp. 101-104.

[5] R. Ansari and B. Liu, "Multirate signal processing", in S. K. Mitra and J. F. Kaiser, Eds., *Handbook for Digital Signal Processing*. New York: John Wiley & Sons, 1993.

[6] D. Babic, J. Vesma, and M. Renfors, "Decimation by irrational factor using CIC-filter and linear interpolation", in *Proc. IEEE Int. Conf. Acoust., Speech, Signal Processing*, Salt Lake City, UT, May 2001.

[7] E. Buracchini, "The software radio concept," *IEEE Commun. Mag.*, vol. 38, pp. 138-143, Sept. 2000.

[8] C. Caballero Gaudes, M. Valkama, M. Renfors, and J. Ajanki, "Fast frequency synthesizer concept based on digital tuning and I/Q signal processing," in *Proc. IEEE Int. Conf. Digital Signal Processing*, Santorini, Greece, July 2002, pp. 1317-1320.

[9] J.-F. Cardoso, "Blind source separation: Statistical principles," *Proc. IEEE*, vol. 86, pp. 2009-2025, Oct. 1998.

[10] J.-F. Cardoso and B. H. Laheld, "Equivariant adaptive source separation," *IEEE Trans. Signal Processing*, vol. 44, pp. 3017-3030, Dec. 1996.

[11] J. K. Cavers and M. W. Liao, "Adaptive compensation for imbalance and offset losses in direct conversion transceivers," *IEEE Trans. Veh. Technol.*, vol. 42, pp. 581-588, Nov. 1993.

[12] E. Cetin, I. Kale, and R. C. S. Morling, "Adaptive compensation of analog front-end I/Q mismatches in digital receivers," in *Proc. IEEE Int. Symp. Circuits Syst.*, Sydney, Australia, May 2001, pp. 370-373.

[13] J. Y. C. Cheah, "Introduction to wireless communications applications and circuit design," in L. E. Larson, Ed., *RF and Microwave Circuit Design for Wireless Communications*. Norwood, MA: Artech House, 1996, pp. 17-41.

[14] C. Chien, *Digital Radio Systems on a Chip – A Systems Approach*. Norwell, MA: Kluwer Academic Publishers, 2001.

[15] S. Choi, A. Cichocki, and S. Amari, "Flexible independent component analysis," in *Proc. IEEE Signal Processing Soc. Workshop Neural Networks Signal Processing*, Cambridge, UK, Aug. 1998, pp. 83-92.

[16] A. J. Coulson, "A generalization of nonuniform bandpass sampling," *IEEE Trans. Signal Processing*, vol. 43, pp. 694-704, Mar. 1995.

[17] A. J. Coulson, R. G. Vaughan, and M. A. Poletti, "Frequency-shifting using bandpass sampling," *IEEE Trans. Signal Processing*, vol. 42, pp. 1556-1559, June 1994.

[18] J. Crols and M. S. J. Steyaert, "An analog integrated polyphase filter for a high performance low-IF receiver," in *IEEE Symp. VLSI Circuits Dig. Tech. Papers*, Kyoto, Japan, June 1995, pp. 87-88.

[19] J. Crols and M. S. J. Steyaert, "A 1.5 GHz highly linear CMOS downconversion mixer," *IEEE J. Solid-State Circuits*, vol. 30, pp. 736-742, July 1995.

[20] J. Crols and M. S. J. Steyaert, "A single-chip 900 MHz CMOS receiver front-end with a high performance low-IF topology," *IEEE J. Solid-State Circuits*, vol. 30, pp. 1483-1492, Dec. 1995.

[21] J. Crols and M. S. J. Steyaert, "Low-IF topologies for high-performance analog front ends of fully integrated receivers," *IEEE Trans. Circuits Syst. II*, vol. 45, pp. 269-282, Mar. 1998.

[22] J. Crols and M. S. J. Steyaert, *CMOS Wireless Transceiver Design*. Dordrecht, the Netherlands: Kluwer Academic Publishers, 1997.

[23] C. Dick and f. harris, "Configurable logic for digital communication: Some signal processing perspectives," *IEEE Commun. Mag*., vol. 37, Aug. 1999.

[24] V. Eerola, T. Ritoniemi, and H. Tenhunen, "Second-order sampling and oversampled A/D- and D/A-converters in digital data transmission," in *Proc. IEEE Int. Symp. Circuits Syst.*, Singapore, June 1991, pp. 1521-1524.

[25] C. W. Farrow, "A continuously variable digital delay element," in *Proc. IEEE Int. Symp. Circuits Syst*., Espoo, Finland, June 1988, pp. 2641-2645.

[26] M. Faulkner, T. Mattsson, and W. Yates, "Automatic adjustment of quadrature modulators," *Electron. Lett*., vol. 27, pp. 214-216, Jan. 1991.

[27] W. Feixue, Y. Shaowei, and G. Guirong, "Mixer-free digital quadrature demodulation based on second-order sampling," *Electron. Lett*., vol. 34, pp. 854-855, Apr. 1998.

[28] M. E. Frerking, *Digital Signal Processing in Communication Systems*. New York: Chapman & Hall, 1994.

[29] A. Gatherer, T. Stetzler, M. McMahan, and E. Auslander, "DSP-based architectures for mobile communications: Past, present and future," *IEEE Commun. Mag.*, vol. 38, pp. 84-90, Jan. 2000.

[30] J. P. F. Glas, "Digital I/Q imbalance compensation in a low-IF receiver," in *Proc. IEEE Global Telecommun. Conf.*, Sydney, Australia, Nov. 1998, pp. 1461-1466.

[31] R. A. Green, "An optimized multi-tone calibration signal for quadrature receiver communication systems," in *Proc. IEEE Workshop Statist. Signal Array Processing*, Pocono Manor, PA, USA, Aug. 2000, pp. 664-667.

[32] R. A. Green, R. Anderson-Sprecher, and J. W. Pierre, "Quadrature receiver mismatch calibration," *IEEE Trans. Signal Processing*, vol. 47, pp. 3130-3133, Nov. 1999.

[33] J. E. Gunn, K. S. Barron, and W. Ruczczyk, "A low-power DSP core-based software radio architecture," *IEEE J. Select. Areas Commun.*, vol. 17, pp. 574-590, Apr. 1999.

[34] S. L. Hahn, *Hilbert Transforms in Signal Processing*. Norwood, MA: Artech House, 1996.

[35] L. Hanzo, "Bandwidth-efficient wireless multimedia communications," *Proc. IEEE*, vol. 86, pp. 1342-1382, July 1998.

[36] f. harris, C. Dick, and M. Rice, "Digital receivers and transmitters using polyphase filter banks for wireless communications," *IEEE Trans. Microwave Theory and Techniques*, vol. 51, pp. 1395-1412, Apr. 2003.

[37] f. harris and M. Rice, "Multirate digital filters for symbol timing synchronization in software defined radios," *IEEE J. Select. Areas Commun.*, vol. 19, pp. 2346-2357, Dec. 2001.

[38] f. harris, "Digital signal processing in radio receivers and transmitters," *Int. J. Wireless Information Networks*, vol. 5, pp. 133-145, 1997.

[39] f. harris, "Digital filter equalization of analog gain and phase mismatch in I-Q receivers," in *Proc. IEEE Int. Conf. Univ. Pers. Commun.*, Cambridge, MA, USA, Sept. 1996, pp. 793-796.

[40] S. Haykin, *Adaptive Filter Theory*, 3rd ed. Upper Saddle River, NJ: Prentice-Hall, 1996.

[41] S. Haykin, Ed., *Unsupervised Adaptive Filtering, vol I: Blind Source Separation*. New York: John Wiley & Sons, 2000.

[42] T. Hentschel and G. Fettweis, "Software radio receivers," in F. Swarts, P. van Rooyan, I. Oppermann, and M. P. Lötter, Eds., *CDMA Techniques for Third Generation Mobile Systems*. Norwell, MA: Kluwer Academic Publishers, 1999, pp. 257-283.

[43] T. Hentschel, M. Henker, and G. Fettweis, "The digital front-end of software radio terminals," *IEEE Pers. Commun.*, vol. 6, pp. 40-46, Aug. 1999.

[44] D. Hilborn, S. P. Stapleton, and J. K. Cavers, "An adaptive direct conversion transmitter," *in Proc. IEEE Veh. Technol. Conf.*, Denver, CO, USA, June 1992, pp. 764-767.

[45] A. Hyvärinen, J. Karhunen, and E. Oja, *Independent Component Analysis*. New York: John Wiley & Sons, 2001.

[46] S. A. Jantzi, K. W. Martin, and A. S. Sedra, "Quadrature bandpass delta-sigma modulation for digital radio," *IEEE J. Solid-State Circuits*, vol. 32, pp. 1935-1950, Dec. 1997.

[47] Y.-C. Jeng, "Perfect reconstruction of digital spectrum from nonuniformly sampled signals," *IEEE Trans. Instrum. Meas.*, vol. 46, pp. 649-652, June 1997.

[48] H. R. Karimi and B. Friedrichs, "Wideband digital receivers for multi-standard software radios," in *IEE Coll. Adaptable Multi-Standard Mobile Radio Terminals*, London, UK, Mar. 1998, pp. 5/1-5/7.

[49] T. E. Kolding, "Multi-standard mixed-signal transceivers for wireless communications – A research overview," Department of Communication Technology, Aalborg University, Aalborg, Denmark, Tech. Rep. R-96-1005, Dec. 1996.

[50] T. I. Laakso, V. Välimäki, M. Karjalainen, and U. K. Laine, "Splitting the unit delay," *IEEE Signal Processing Mag*., vol. 13, pp. 30-60, Jan. 1996.

[51] E. A. Lee and D. G. Messerschmitt, *Digital Communication*. Boston, MA: Kluwer Academic Publishers, 1988.

[52] J. P. Y. Lee, "Wideband I/Q demodulators: Measurement technique and matching characteristics," *IEE Proc. Radar, Sonar, Navigation*, vol. 143, pp. 300-306, Oct. 1996.

[53] Y.-P. Lin and P. P. Vaidyanathan, "Periodically nonuniform sampling of bandpass signals," *IEEE Trans. Circuits Syst. II*, vol. 45, pp. 340-351, Mar. 1998.

[54] A. Lohtia, P. A. Gould, and C. G. Englefield, "An adaptive digital technique for compensating for analog quadrature modulator / demodulator impairments," *in Proc. IEEE Pacific Rim Conf. Commun., Comput., Signal Processing*, Victoria, BC, Canada, May 1993, pp. 447-450.

[55] W. W. Lu, "Compact multidimensional broadband wireless: The convergence of wireless mobile and access," *IEEE Commun. Mag.*, vol. 38, pp. 119-123, Nov. 2000.

[56] H. Meyr, M. Moeneclay, and S. A. Fechtel, *Digital Communication Receivers*. New York: John Wiley & Sons, 1998.

[57] S. Mirabbasi and K. Martin, "Classical and modern receiver architectures," *IEEE Commun. Mag.*, vol. 38, pp. 132-139, Nov. 2000.

[58] R. L. Mitchell, "Creating complex signal samples from a band-limited real signal," *IEEE Trans. Aerosp. Electron. Syst.*, vol. 25, pp. 425-427, May 1989.

[59] J. Mitola, *Software Radio Architecture: Object-Oriented Approaches to Wireless Systems Engineering*. New York: John Wiley & Sons, 2000.

[60] H. Nguyen, "Improving QPSK demodulator performance for quadrature receiver with information from amplitude and phase imbalance correction," *in Proc. IEEE Wireless Commun. Networking Conf.*, Chicago, IL, USA, Sept. 2000, pp. 1440-1444.

[61] T. Okanobu, H. Tomiyama, and H. Arimoto, "Advanced low voltage single chip radio IC," *IEEE Trans. Consumer Electron.*, vol. 38, pp. 465-475, Aug. 1992.

[62] J. M. Paez-Borrallo and F. J. Casajus Quiros, "Self adjusting digital image rejection receiver for mobile communications," *in Proc. IEEE Veh. Technol. Conf.*, Phoenix, AZ, USA, May 1997, pp. 686-690.

[63] J. W. Pierre and D. R. Fuhrmann, "Considerations in the autocalibration of quadrature receivers," in *Proc. IEEE Int. Conf. Acoust., Speech, Signal Processing*, Detroit, MI, USA, May 1995, pp. 1900-1903.

[64] R. Porat and f. harris, "Resolving and correcting gain and phase mismatch in transmitters and receivers for wideband ofdm systems," in *Proc. Asilomar Conf. Signals, Syst., Computers*, Pacific Grove, CA, Nov. 2002, pp. 1005-1009.

[65] K.-P. Pun, J. E. Franca, and C. Azeredo-Leme, "Wideband digital correction of I and Q mismatch in quadrature radio receivers," in *Proc. IEEE Int. Symp. Circuits Syst.*, Geneva, Switzerland, May 2000, pp. 661-664.

[66] C. M. Rader, "A simple method for sampling in-phase and quadrature components," *IEEE Trans. Aerosp. Electron. Syst.*, vol. 20, pp. 821-824, Nov. 1984.

[67] T. S. Rappaport, *Wireless Communications: Principles and Practice*. Upper Saddle River, NJ: Prentice-Hall, 1996.

[68] B. Razavi, "Design considerations for direct-conversion receivers," *IEEE Trans. Circuits Syst. II*, vol. 44, pp. 428-435, June 1997.

[69] B. Razavi, "RF IC design challenges," in *Proc. Design Autom. Conf.*, San Francisco, CA, USA, June 1998, pp. 408-413.

[70] U. L. Rohde, J. Whitaker, and T. T. N. Bucher, *Communications Receivers: Principles and Design*, 2nd ed. New York: McGraw-Hill, 1997.

[71] S. J. Roome, "Analysis of quadrature detectors using complex envelope notation," *IEE Proc. Radar and Signal Processing*, vol. 136, pp. 95-100, Apr. 1989.

[72] J. C. Rudell *et al*., "A 1.9-GHz wide-band IF double conversion CMOS receiver for cordless telephone applications," *IEEE J. Solid-State Circuits*, vol. 32, pp. 2071-2088, Dec. 1997.

[73] J. Sevenhans, B. Verstraeten, and S. Taraborrelli, "Trends in silicon radio large scale integration: Zero IF receiver! Zero I&Q transmitter! Zero discrete passives!," *IEEE Commun. Mag.*, vol. 38, pp. 142-147, Jan. 2000.

[74] D. K. Shaeffer and T. H. Lee, *The Design and Implementation of Low-Power CMOS Radio Receivers*. Boston, MA: Kluwer Academic Publishers, 1999.

[75] E. Song, S.-I. Chae, and W. Kim, "A 2 GHz CMOS double conversion downconverter with robust image rejection performance against the process and temperature variations," in *IEEE Symp. VLSI Circuits Dig. Tech. Papers*, Honolulu, HI, USA, June 2000, pp. 38-41.

[76] M. S. J. Steyaert and R. Roovers, "A 1-GHz single-chip quadrature modulator," *IEEE J. Solid-State Circuits*, vol. 27, pp. 1194-1197, Aug. 1992.

[77] M. S. J. Steyaert *et al*., "A 2-V CMOS cellular transceiver front-end," *IEEE J. Solid-State Circuits*, vol. 35, pp. 1895-1907, Dec. 2000.

[78] J. Tsui, *Digital Techniques for Wideband Receivers*. Norwood, MA: Artech House, 1995.

[79] H. Tsurumi and Y. Suzuki, "Broadband RF stage architecture for software-defined radio in handheld terminal applications," *IEEE Commun. Mag.*, vol. 37, pp. 90-95, Feb. 1999.

[80] H. Tsurumi *et al*., "Broadband and flexible receiver architecture for software defined radio terminal using direct conversion and low-IF principle," *IEICE Trans. Commun.*, vol. E83-B, pp. 1246-1253, June 2000.

[81] M. Valkama, *Advanced I/Q Signal Processing for Wideband Receivers: Models and Algortihms*. Ph.D. Dissertation, Tampere, Finland: Tampere University of Technology, Dec. 2001.

[82] M. Valkama, M. Renfors, and V. Koivunen, "Advanced methods for I/Q imbalance compensation in communication receivers," *IEEE Trans. Signal Processing*, vol. 49, pp. 2335-2344, Oct. 2001.

[83] M. Valkama, J. Pirskanen, and M. Renfors, "Signal processing challenges for applying software radio principles in future wireless terminals: An overview," *Int. J. Commun. Syst.*, vol. 15, pp. 741-769, Oct. 2002.

[84] M. Valkama and M. Renfors, "A novel image rejection architecture for quadrature radio receivers," *IEEE Trans. Circuits Syst. II*, to appear.

[85] M. Valkama and M. Renfors, "Advanced DSP for I/Q imbalance compensation in a low-IF receiver," in *Proc. IEEE Int. Conf. Communications*, New Orleans, LA, June 2000, pp. 768-772.

[86] M. Valkama, M. Renfors, and V. Koivunen, "Blind source separation based I/Q imbalance compensation," in *Proc. IEEE Symposium 2000 on Adaptive Systems for Signal Processing, Communications and Control*, Lake Louise, AL, Canada, Oct. 2000, pp. 310-314.

[87] M. Valkama, M. Renfors, and V. Koivunen, "Compensation of frequency-selective I/Q imbalances in wideband receivers: Models and algorithms," in *Proc. Third IEEE Signal Processing Workshop Signal Processing Adv. Wireless Commun.*, Taoyuan, Taiwan, R.O.C., March 2001, pp. 42-45.

[88] M. Valkama and M. Renfors, "Second-order sampling of wideband signals," in *Proc. IEEE Int. Symp. Circuits Syst.*, Sydney, Australia, May 2001, pp. 801-804.

[89] R. G. Vaughan, N. L. Scott, and D. R. White, "The theory of bandpass sampling," *IEEE Trans. Signal Processing*, vol. 39, pp. 1973-1984, Sept. 1991.

[90] J. A. Weppman, "Analog-to-digital converters and their applications in radio receivers," *IEEE Commun. Mag.*, vol. 33, pp. 39-45, May 1995.

[91] S. Wu and B. Razavi, "A 900-MHz/1.8-GHz CMOS receiver for dual-band applications," *IEEE J. Solid-State Circuits*, vol. 33, pp. 2178-2185, Dec. 1998.

[92] D. T. S. Yim and C. C. Ling, "A 200-MHz CMOS I/Q downconverter," *IEEE Trans. Circuits Syst. II*, vol. 46, pp. 808-810, June 1999.

[93] L. Yu and W. M. Snelgrove, "A novel adaptive mismatch cancellation system for quadrature IF radio receivers," *IEEE Trans. Circuits Syst. II*, vol. 46, pp. 789-801, June 1999.

[94] K. C. Zangi and R. D. Koilpillai, "Software radio issues in cellular base stations," *IEEE J. Select. Areas Commun.*, vol. 17, pp. 561-573, Apr. 1999.

[95] M. Zeng, A. Annamalai, and V. K. Bhargava, "Recent advances in cellular wireless Communications," *IEEE Commun. Mag.*, vol. 37, pp. 128-138, Sept. 1999.